A night photograph of a large, multi-story building with a red roof and arched windows, situated on a hillside overlooking a body of water. The building is illuminated from within, and its lights reflect on the water. In the background, a white tower with a green dome is visible against the dark sky. The water in the foreground is calm, showing clear reflections of the lights and the building.

Quantum phases of antiferromagnets and the underdoped cuprates

Talk online: sachdev.physics.harvard.edu



Outline

1. Coupled dimer antiferromagnets

Landau-Ginzburg quantum criticality

2. Spin liquids and valence bond solids

(a) Schwinger-boson mean-field theory - square lattice

(b) Gauge theories of perturbative fluctuations

(c) Non-perturbative effects: Berry phases

*(d) Schwinger-boson mean-field theory -
triangular lattice*

(e) Visons and the Kitaev model


3. Cuprate superconductivity

(a) Review of experiments, old and new

(b) Fermi surfaces and the spin density wave theory

(c) Fermi pockets and the underdoped cuprates

References

 Exotic phases and quantum phase transitions: model systems and experiments, Rapporteur talk at the 24th Solvay Conference on Physics, "Quantum Theory of Condensed Matter", arXiv:0901.4103

 Quantum magnetism and criticality, *Nature Physics* **4**, 173 (2008), arXiv:0711.3015

 Quantum phases and phase transitions of Mott insulators, arXiv:cond-mat/0401041

Outline

1. Coupled dimer antiferromagnets

Landau-Ginzburg quantum criticality

2. Spin liquids and valence bond solids

(a) Schwinger-boson mean-field theory - square lattice

(b) Gauge theories of perturbative fluctuations

(c) Non-perturbative effects: Berry phases

*(d) Schwinger-boson mean-field theory -
triangular lattice*

(e) Visons and the Kitaev model

3. Cuprate superconductivity

(a) Review of experiments, old and new

(b) Fermi surfaces and the spin density wave theory

(c) Fermi pockets and the underdoped cuprates

Outline

1. Coupled dimer antiferromagnets

Landau-Ginzburg quantum criticality

2. Spin liquids and valence bond solids

(a) Schwinger-boson mean-field theory - square lattice

(b) Gauge theories of perturbative fluctuations

(c) Non-perturbative effects: Berry phases

*(d) Schwinger-boson mean-field theory -
triangular lattice*

(e) Visons and the Kitaev model

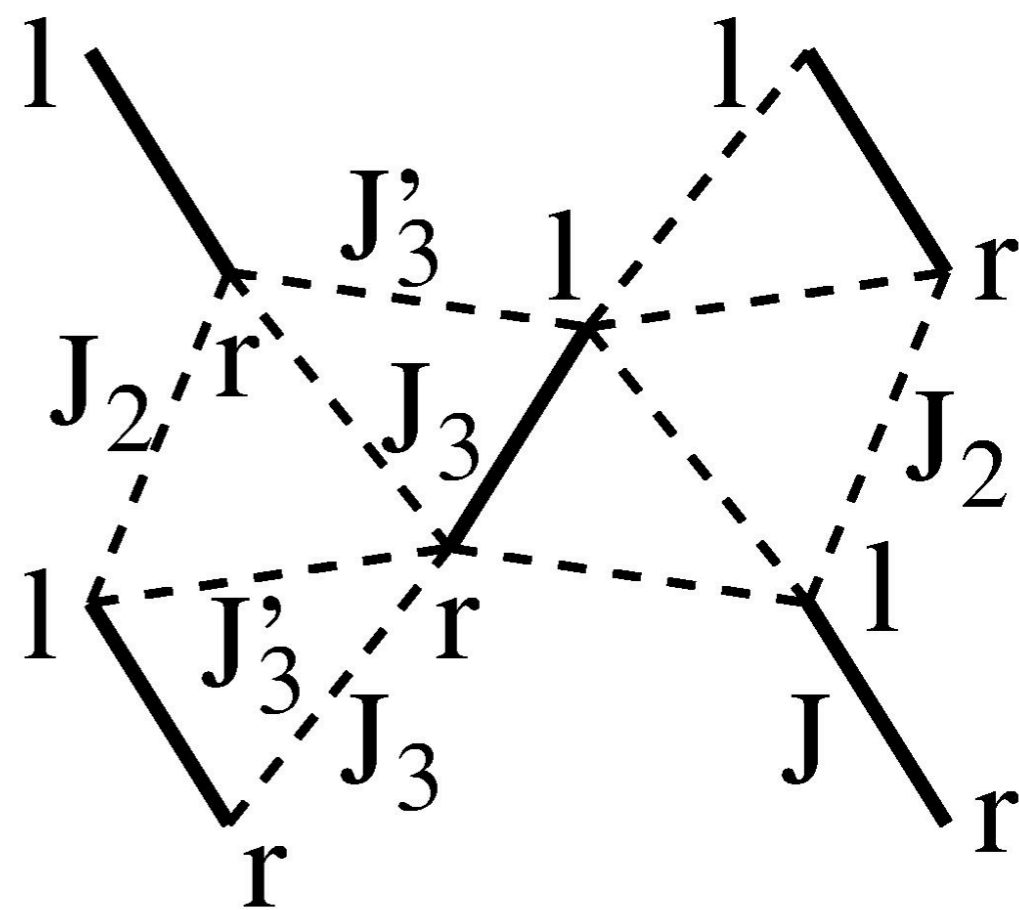
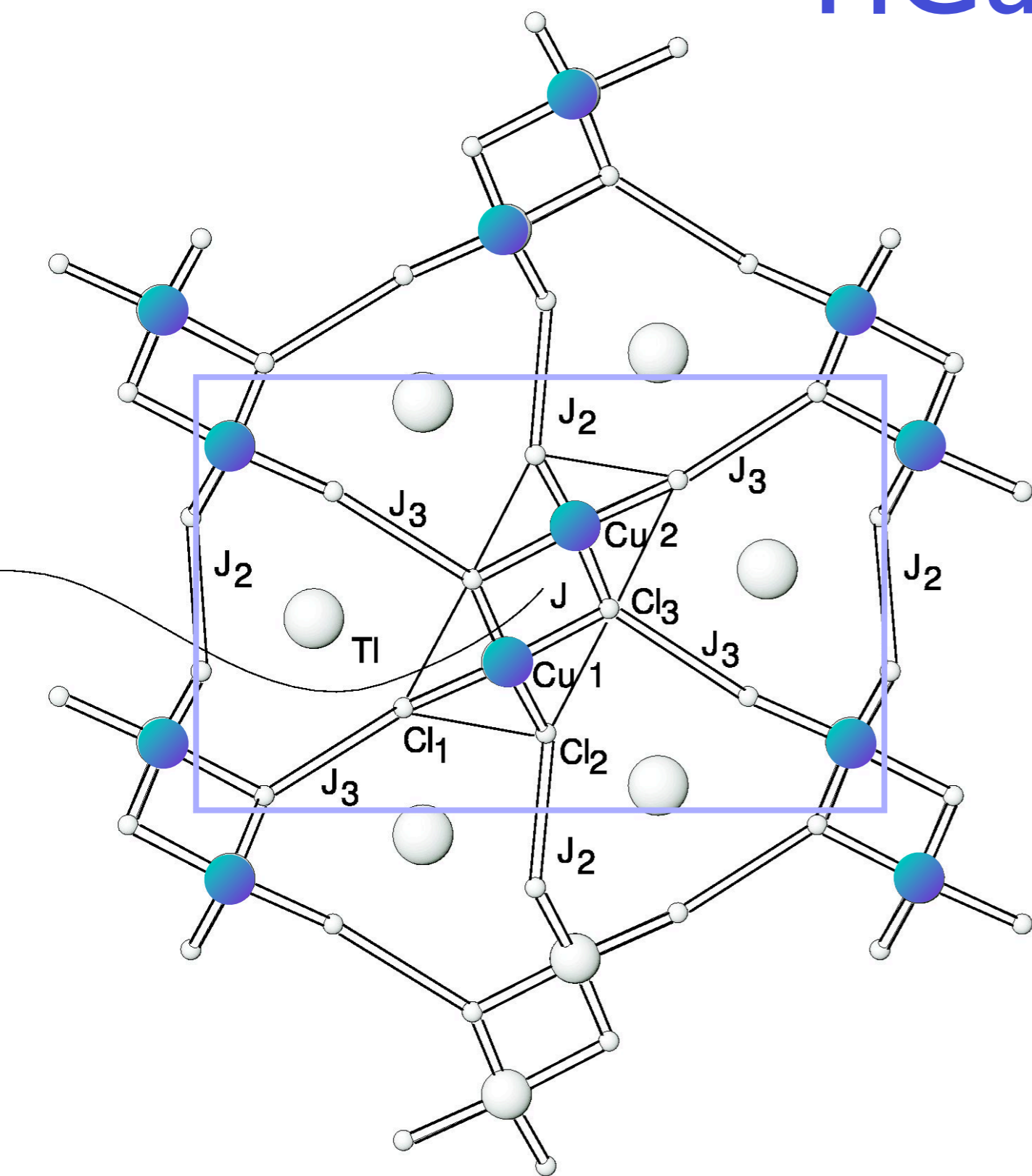
3. Cuprate superconductivity

(a) Review of experiments, old and new

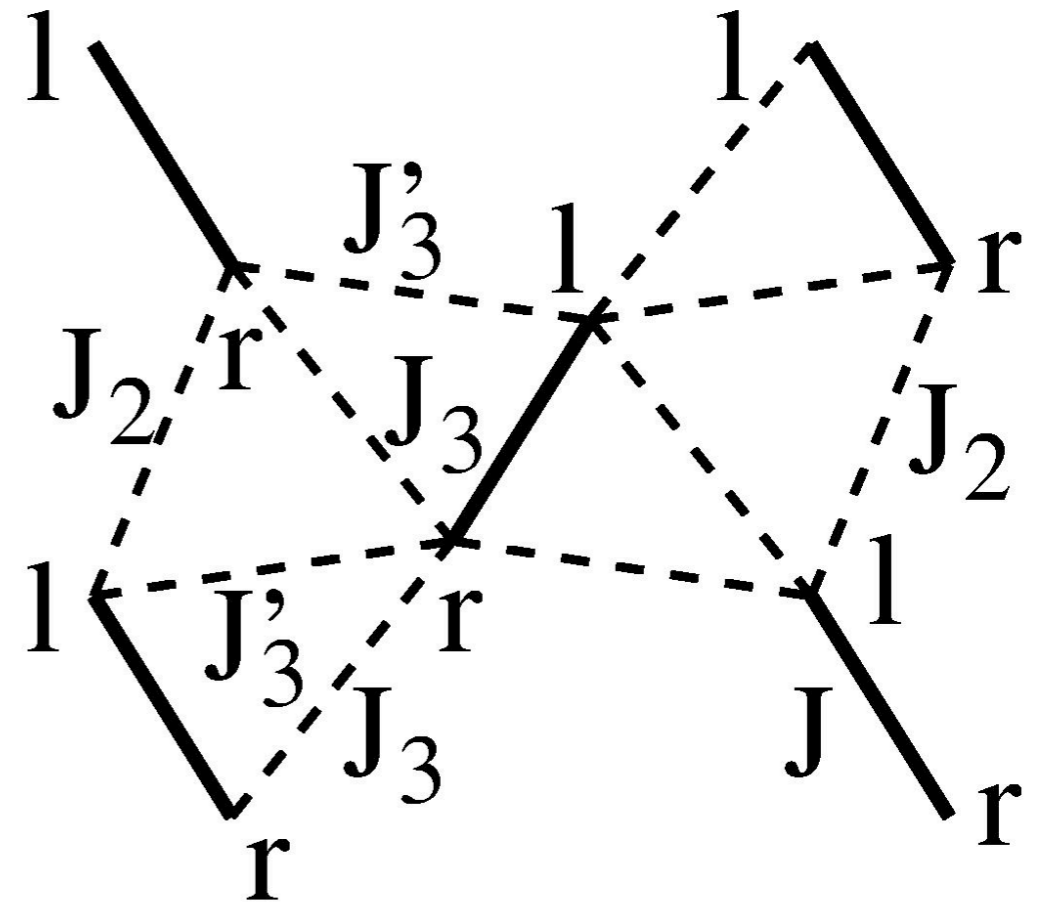
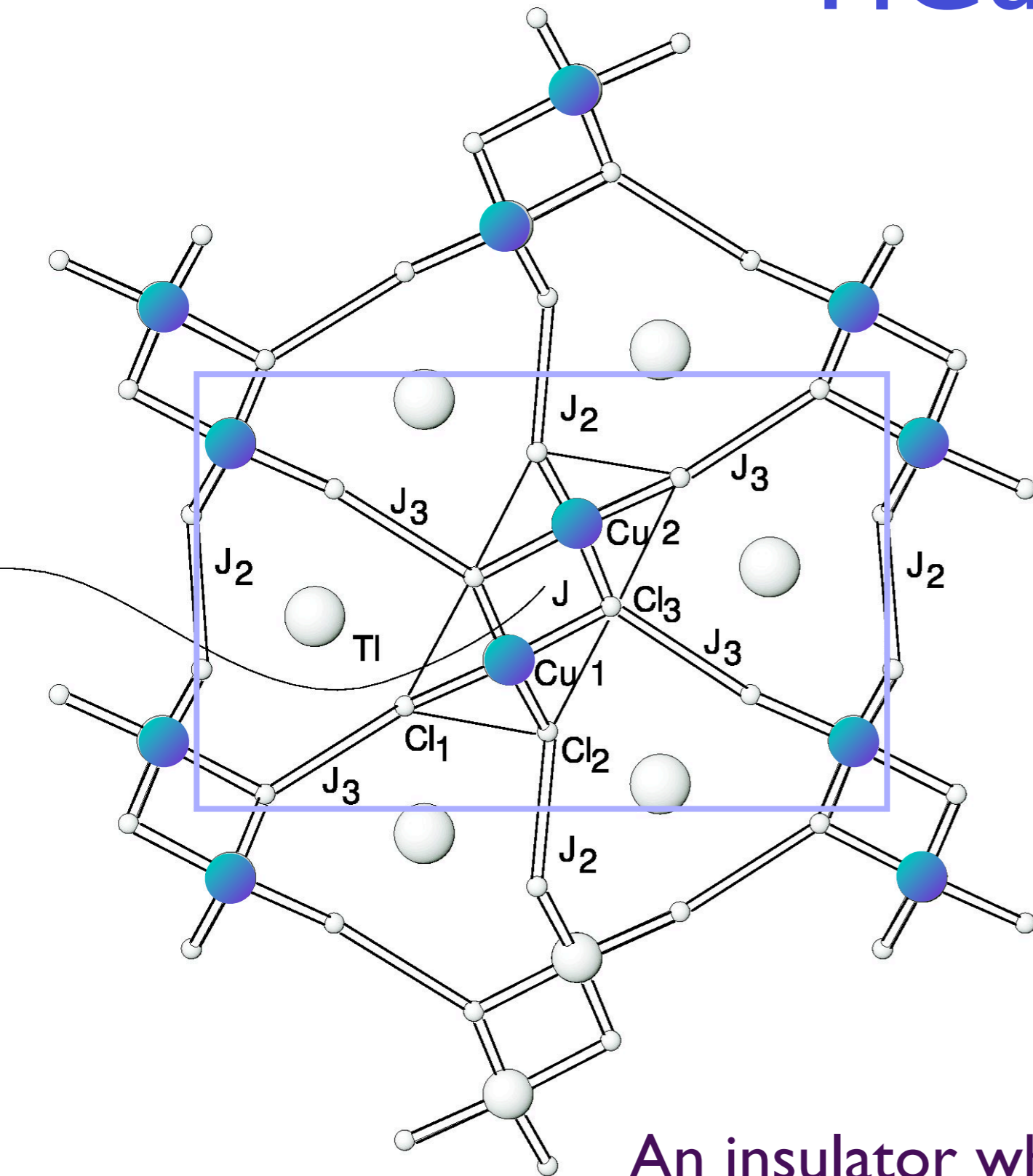
(b) Fermi surfaces and the spin density wave theory

(c) Fermi pockets and the underdoped cuprates

TlCuCl₃



TiCuCl₃



An insulator whose spin susceptibility vanishes exponentially as the temperature T tends to zero.

TlCuCl₃ at ambient pressure

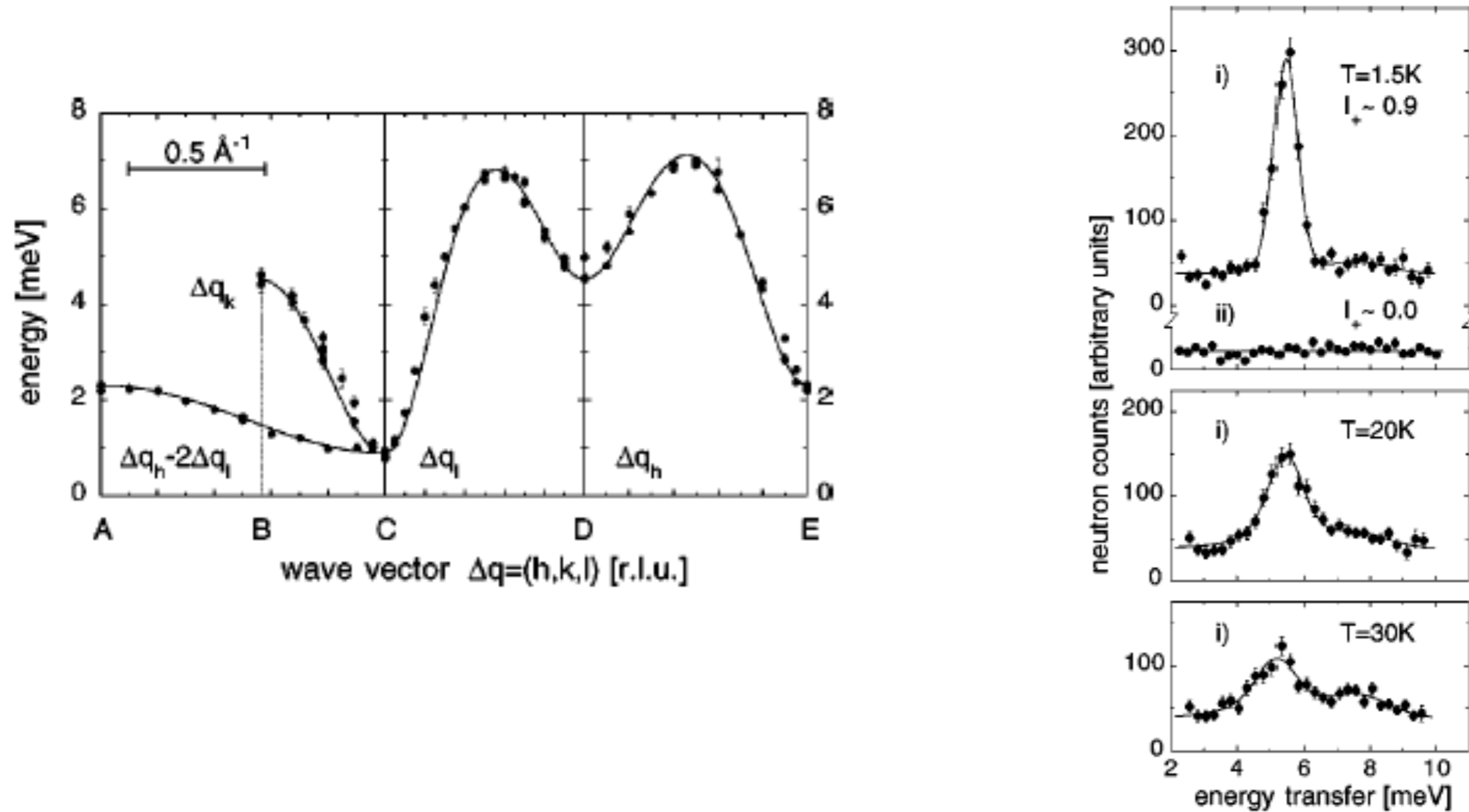
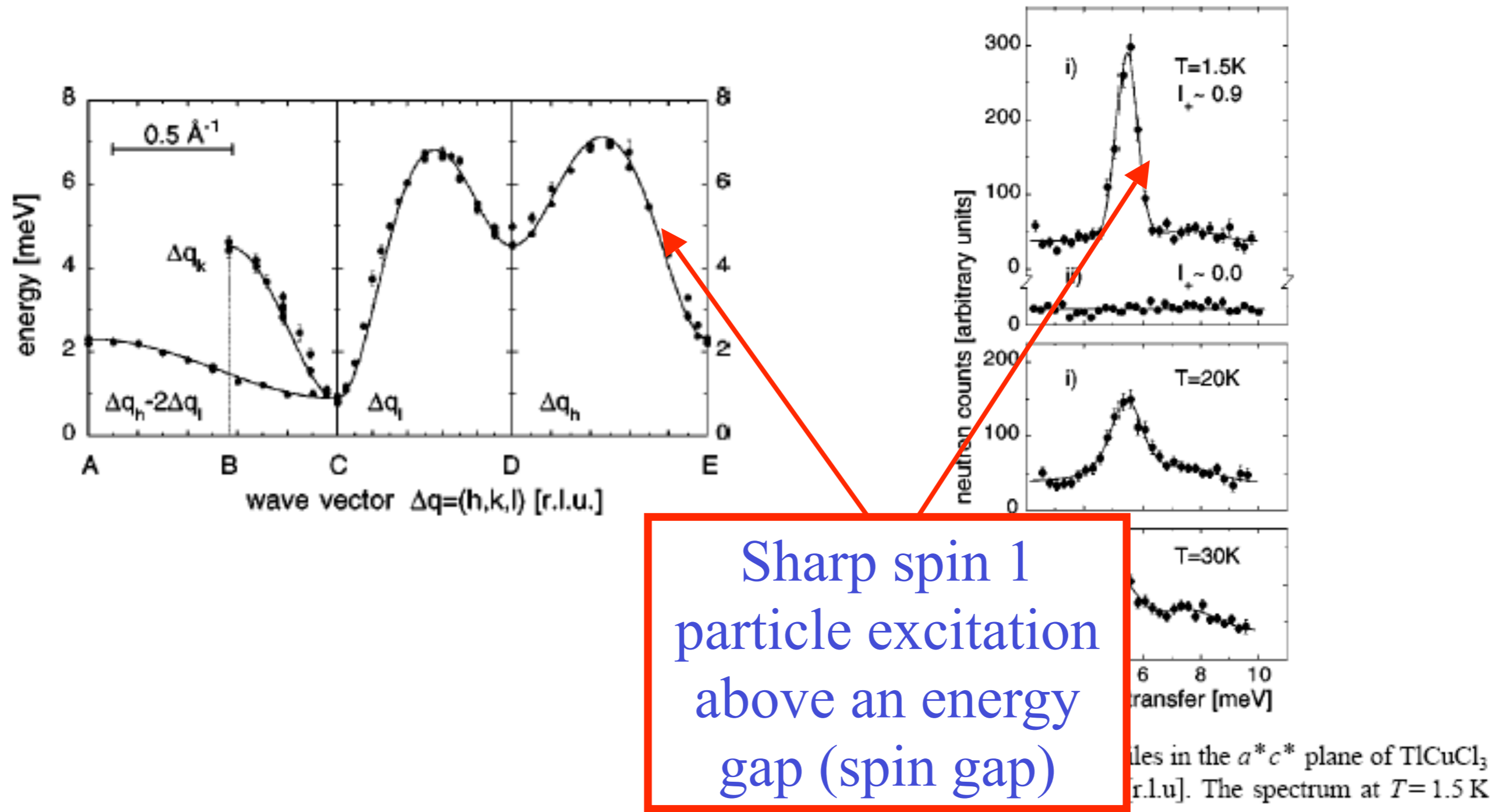


FIG. 1. Measured neutron profiles in the a^*c^* plane of TlCuCl₃ for $i = (1.35, 0, 0)$, $ii = (0, 0, 3.15)$ [r.l.u.]. The spectrum at $T = 1.5 \text{ K}$

N. Cavadini, G. Heigold, W. Henggeler, A. Furrer, H.-U. Güdel, K. Krämer and H. Mutka, *Phys. Rev. B* 63 172414 (2001).

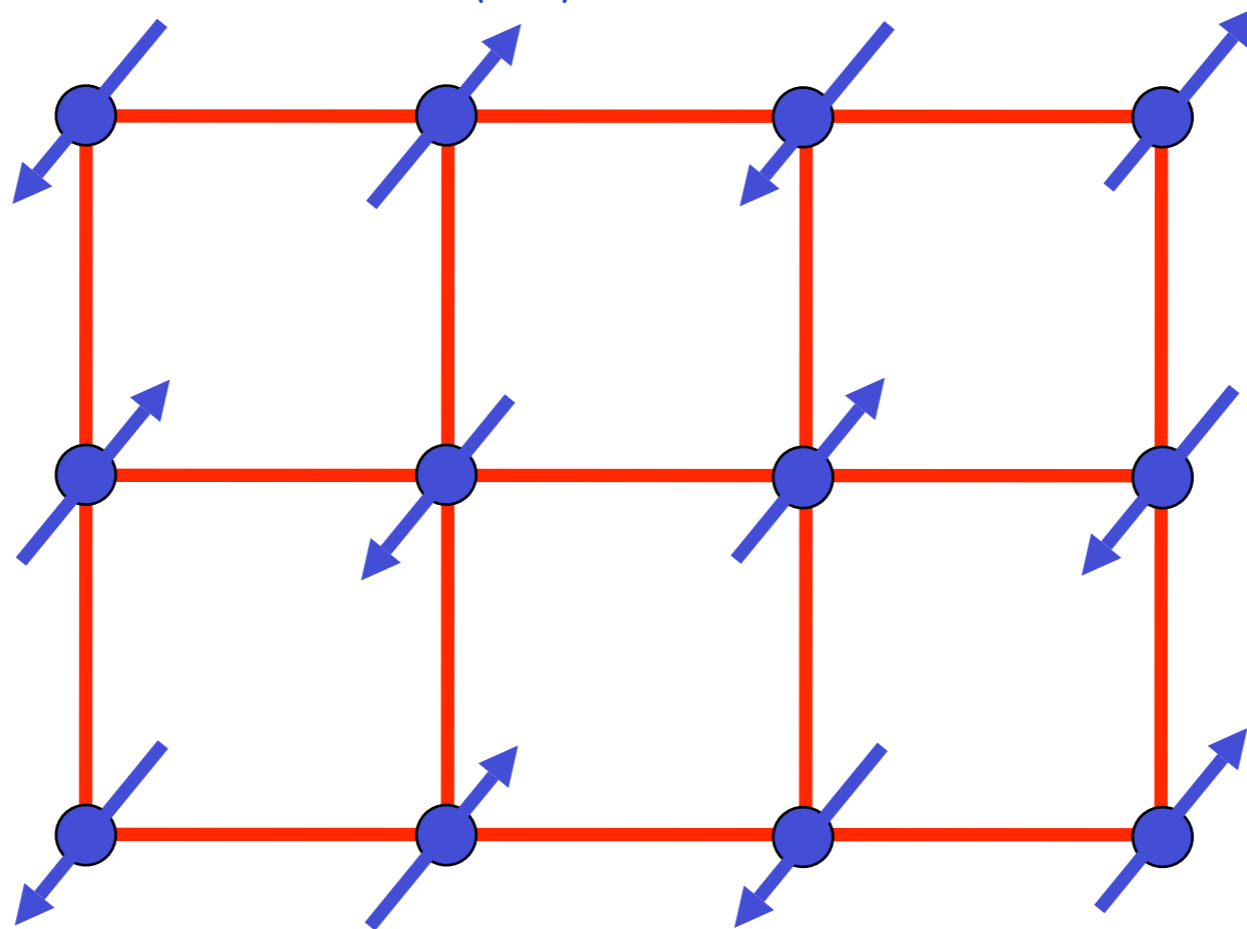
TlCuCl₃ at ambient pressure



N. Cavadini, G. Heigold, W. Henggeler, A. Furrer, H.-U. Güdel, K. Krämer and H. Mutka, *Phys. Rev. B* 63 172414 (2001).

Square lattice antiferromagnet

$$H = \sum_{\langle ij \rangle} J_{ij} \vec{S}_i \cdot \vec{S}_j$$



Ground state has long-range Néel order

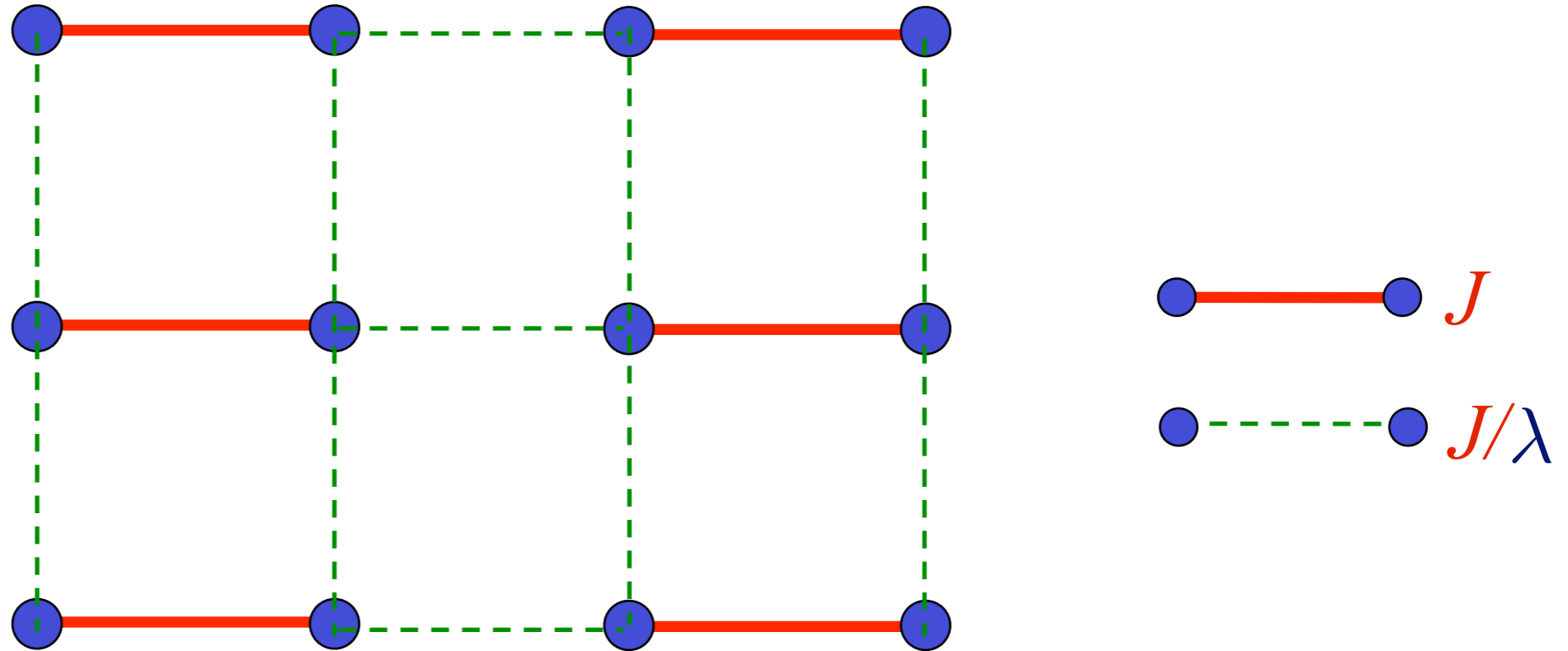
Order parameter is a single vector field $\vec{\varphi} = \eta_i \vec{S}_i$

$\eta_i = \pm 1$ on two sublattices

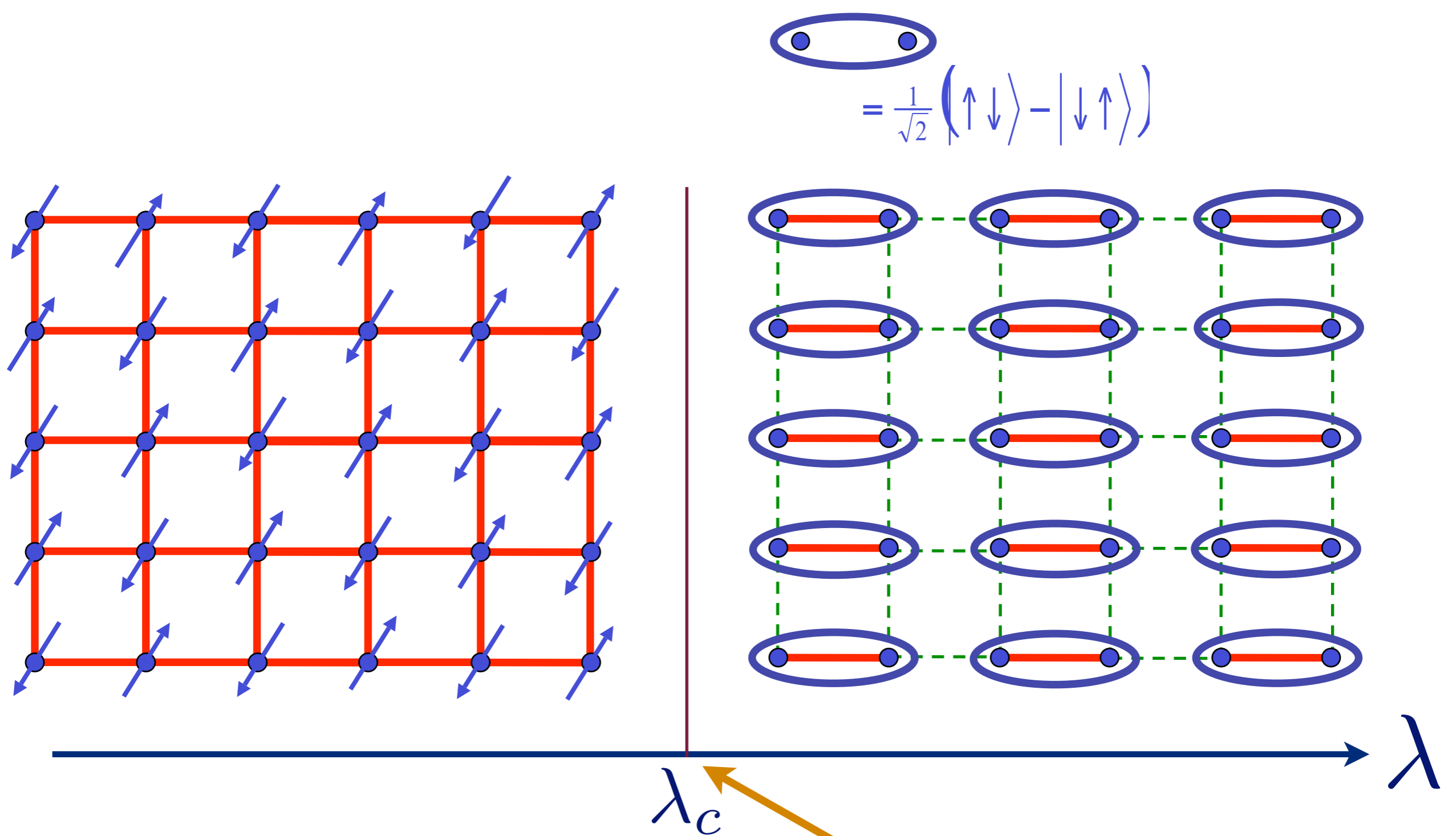
$\langle \vec{\varphi} \rangle \neq 0$ in Néel state.

Square lattice antiferromagnet

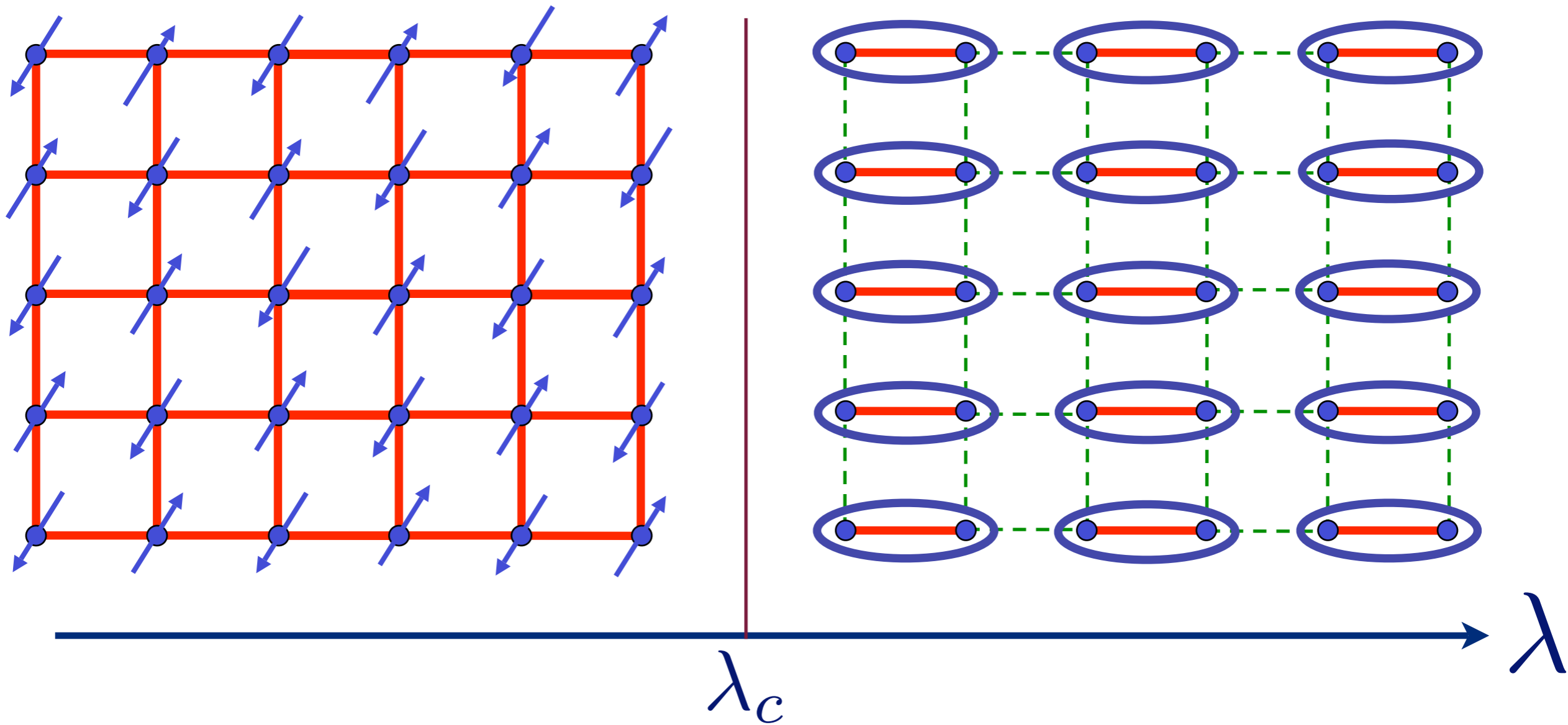
$$H = \sum_{\langle ij \rangle} J_{ij} \vec{S}_i \cdot \vec{S}_j$$



Weaken some bonds to induce spin entanglement in a new quantum phase

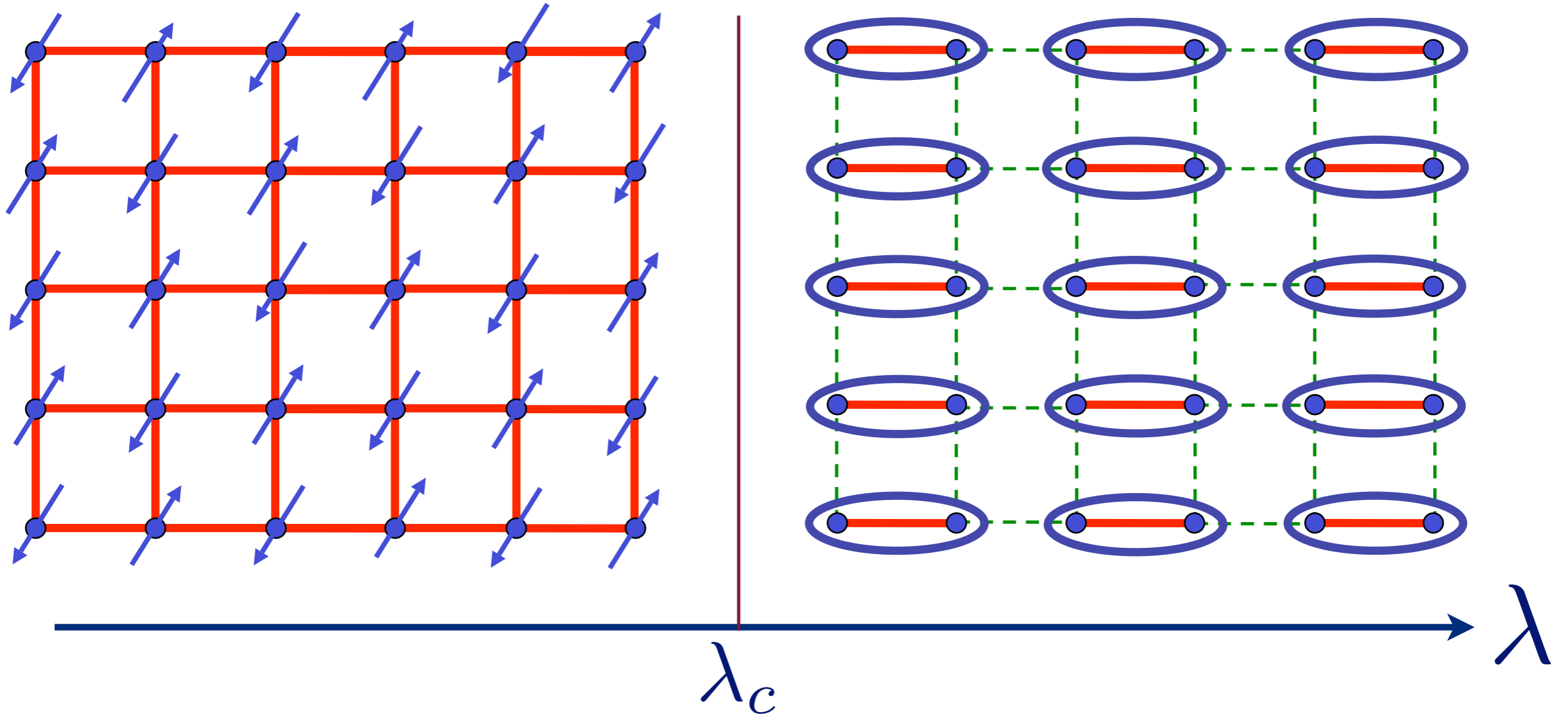


Quantum critical point with non-local entanglement in spin wavefunction

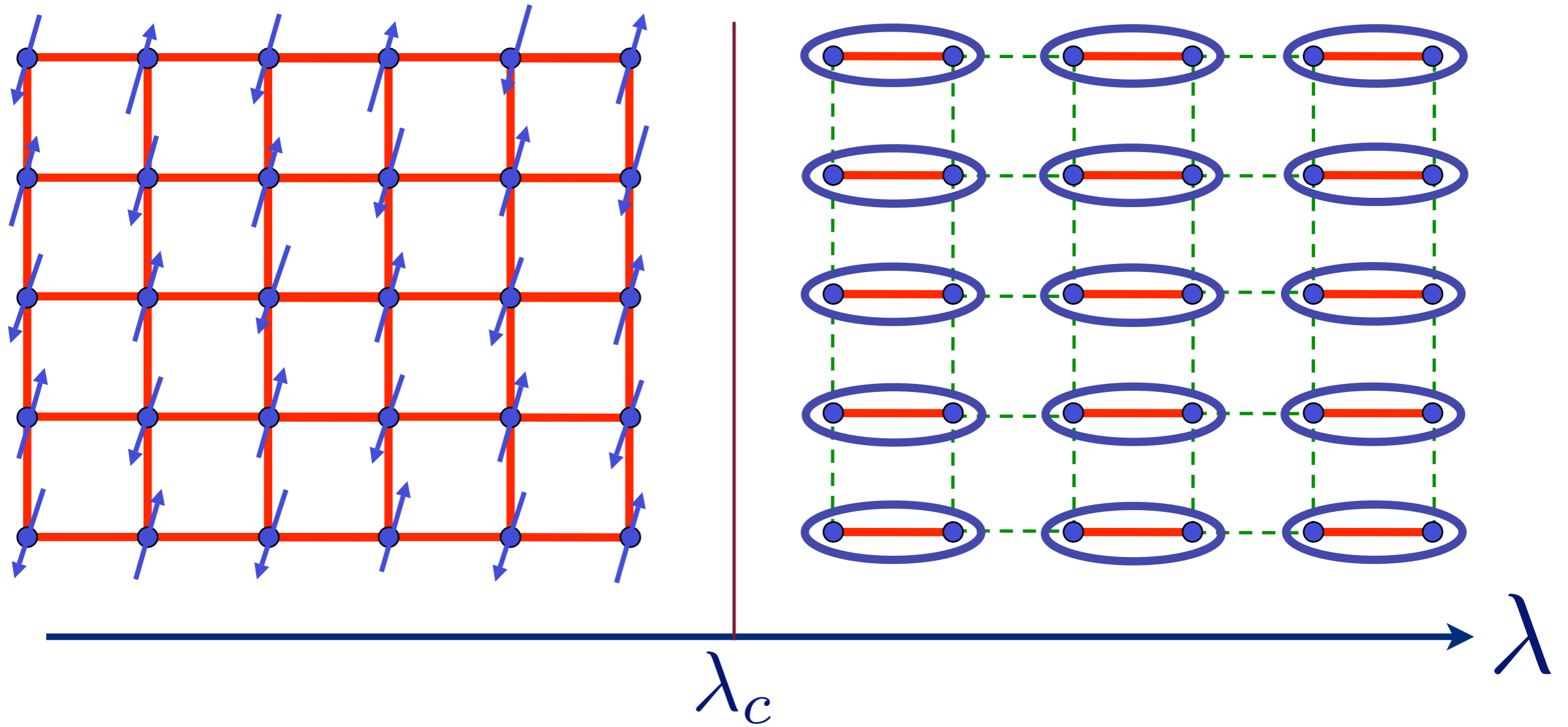


← Pressure in TlCuCl_3

Excitation spectrum in the Néel phase

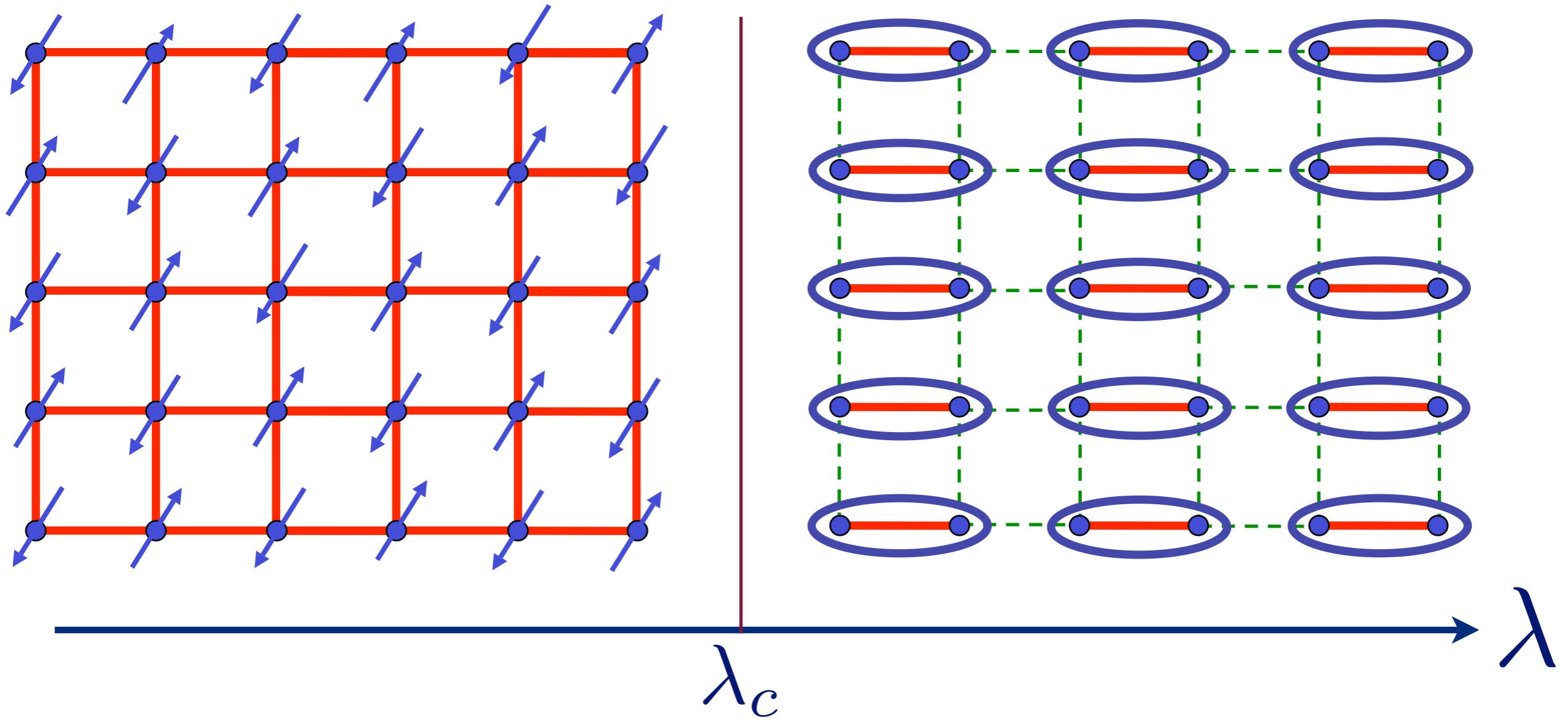


Excitation spectrum in the Néel phase



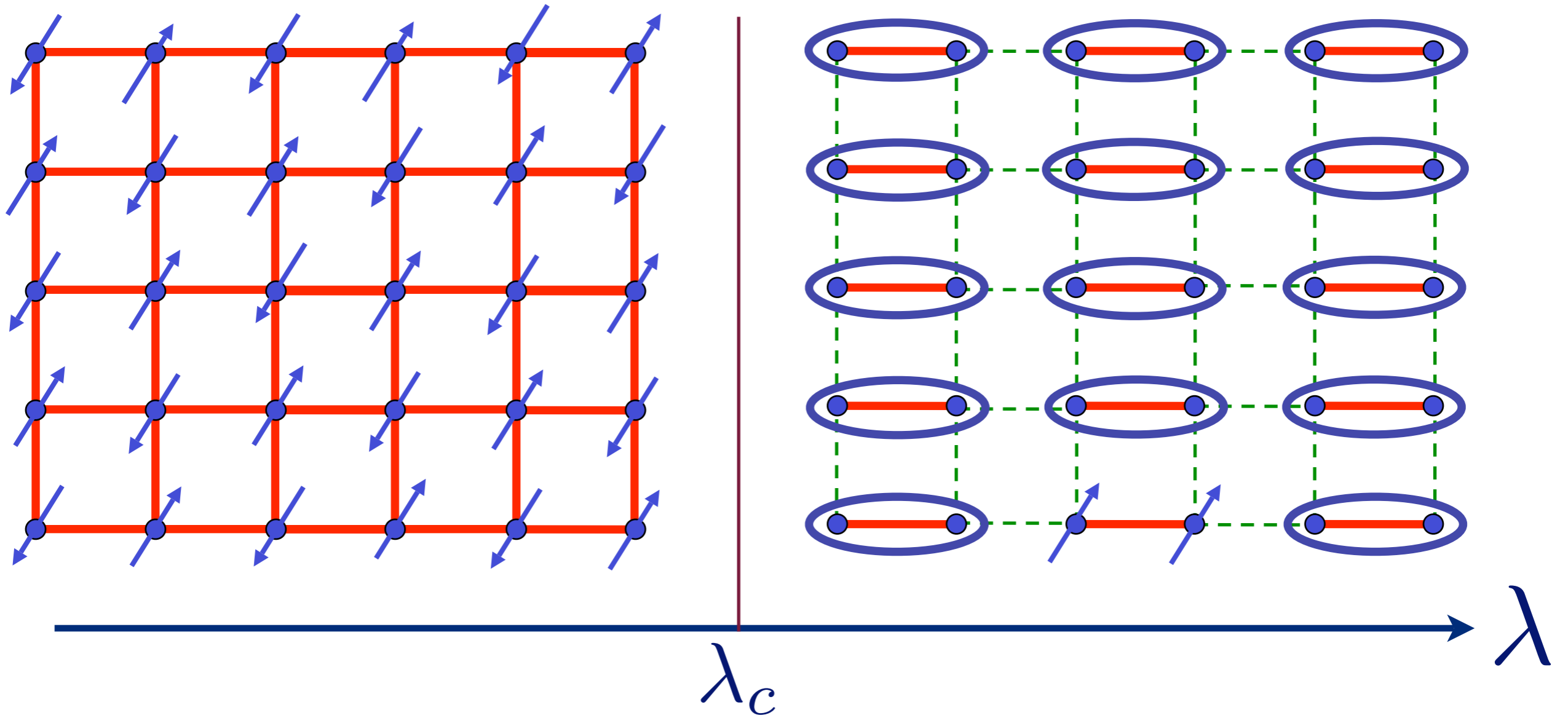
Spin waves

Excitation spectrum in the Néel phase

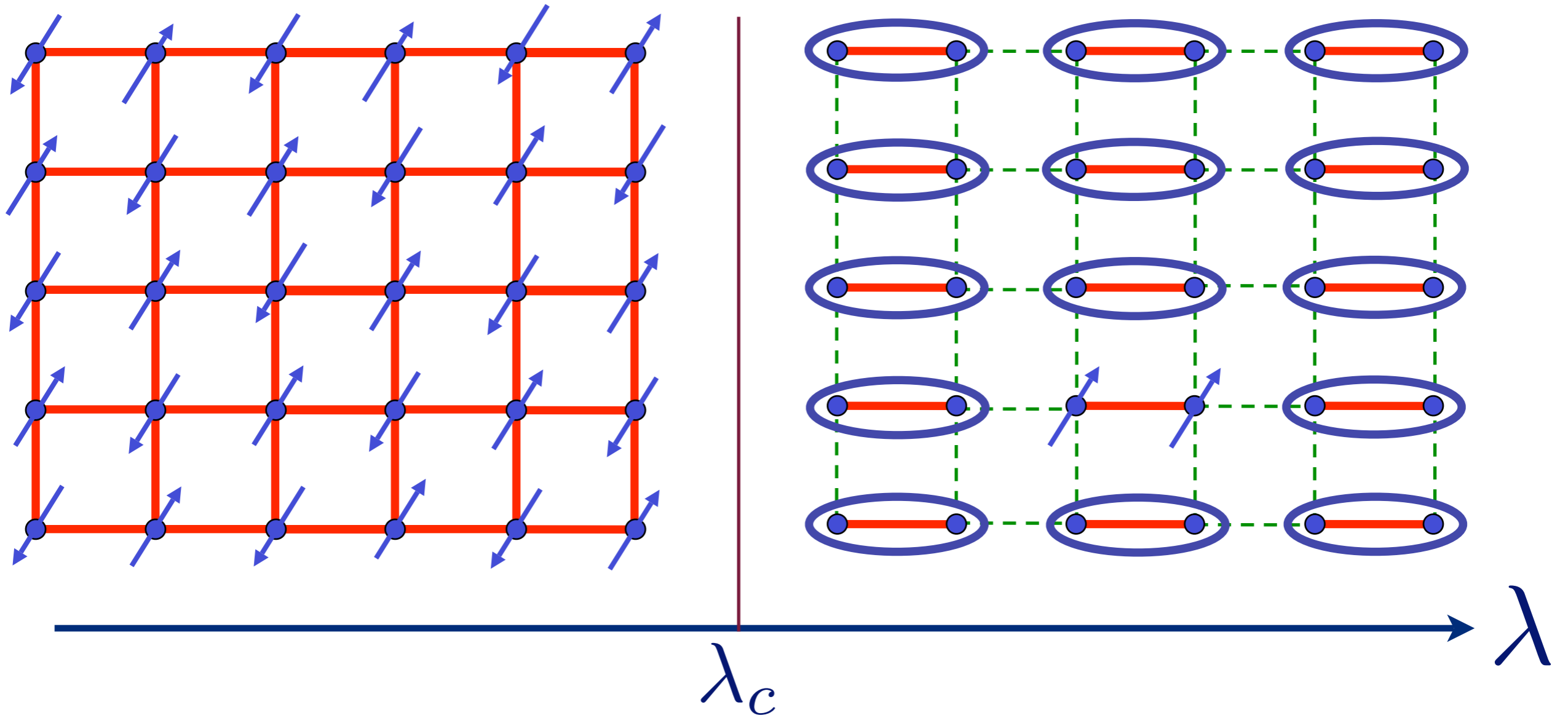


Spin waves

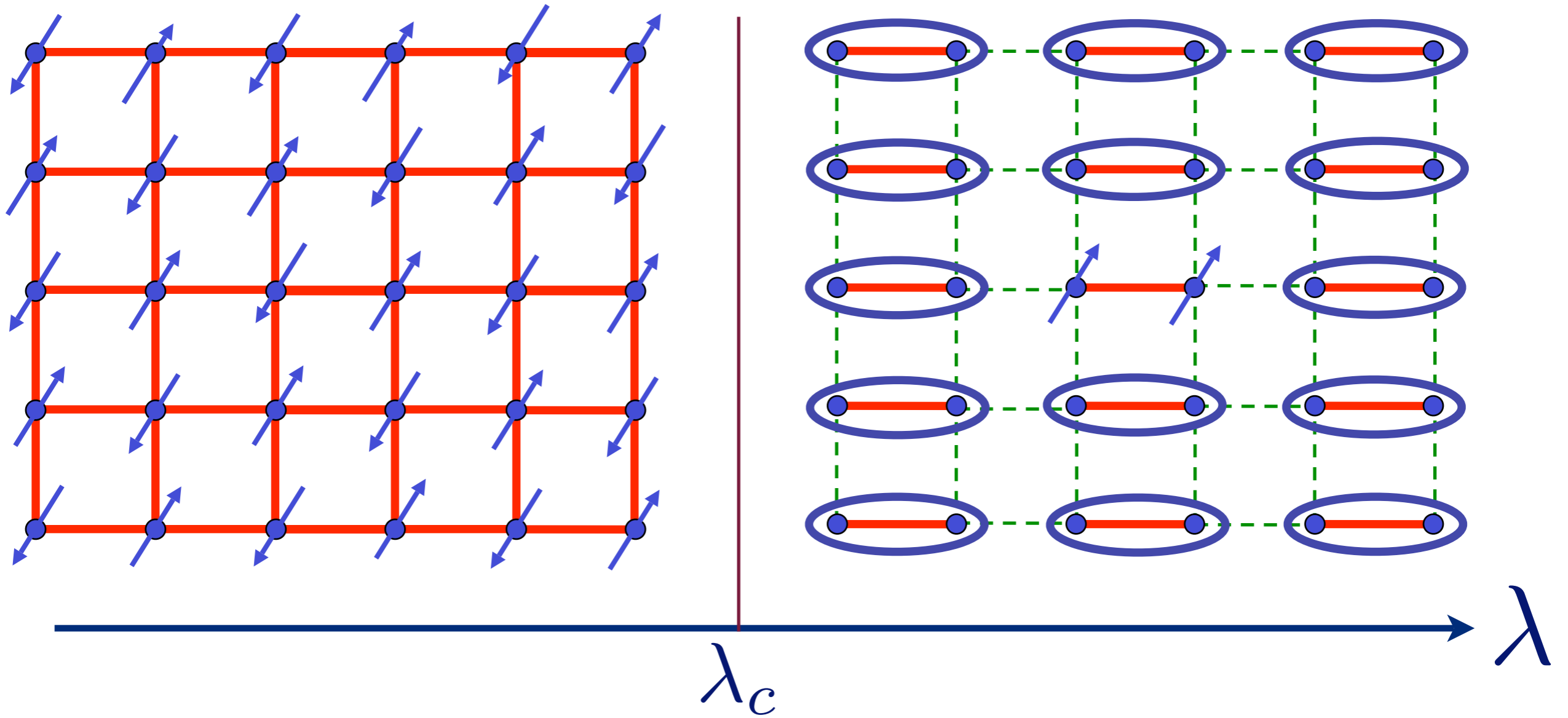
Excitation spectrum in the paramagnetic phase



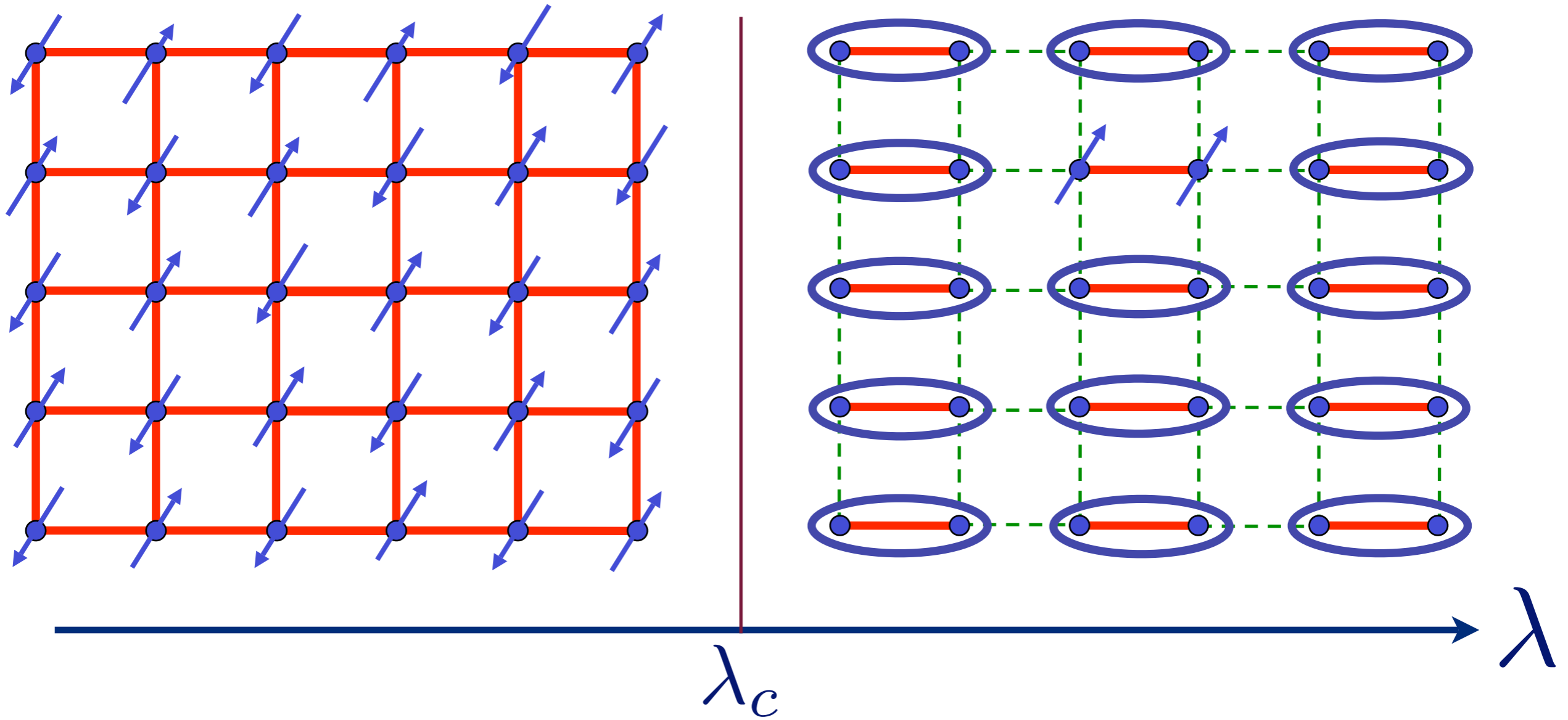
Excitation spectrum in the paramagnetic phase



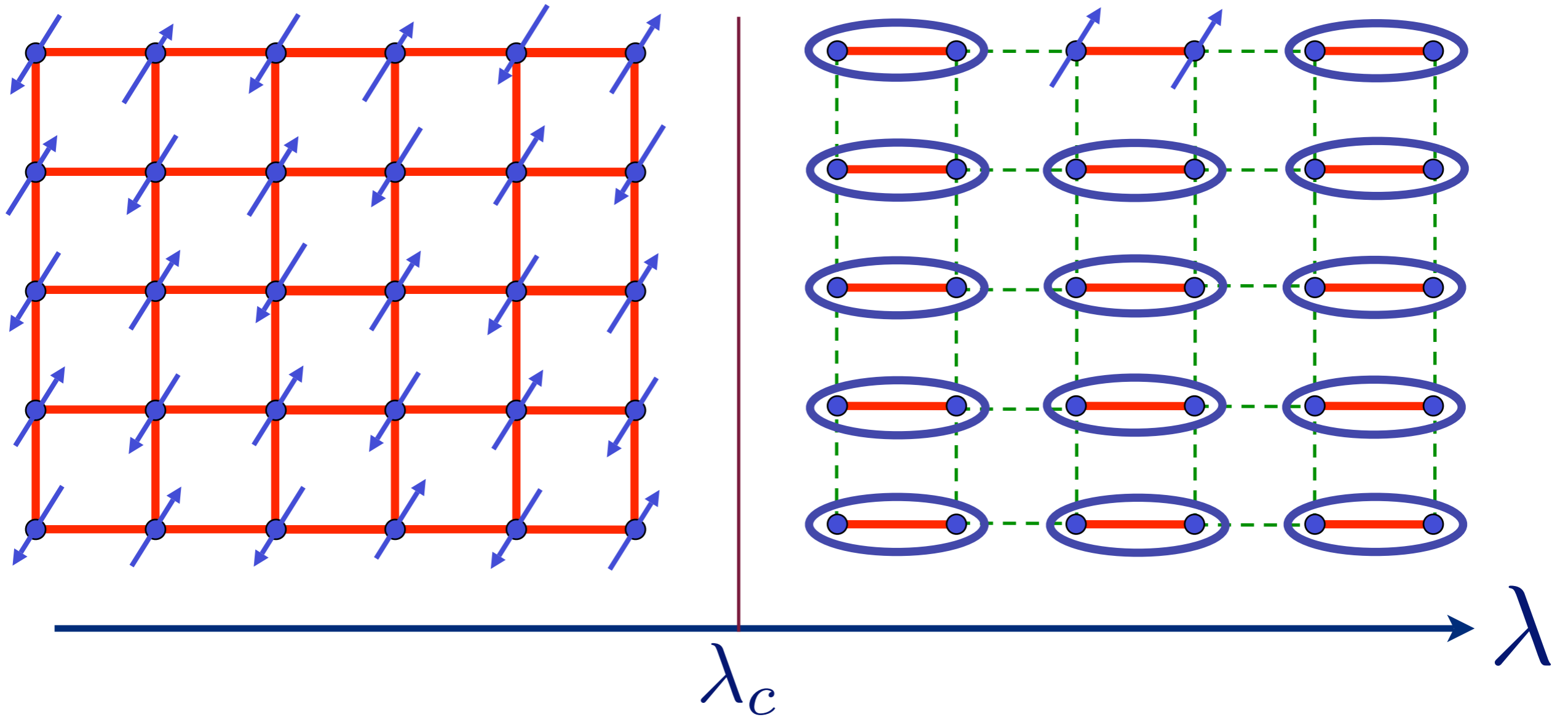
Excitation spectrum in the paramagnetic phase



Excitation spectrum in the paramagnetic phase

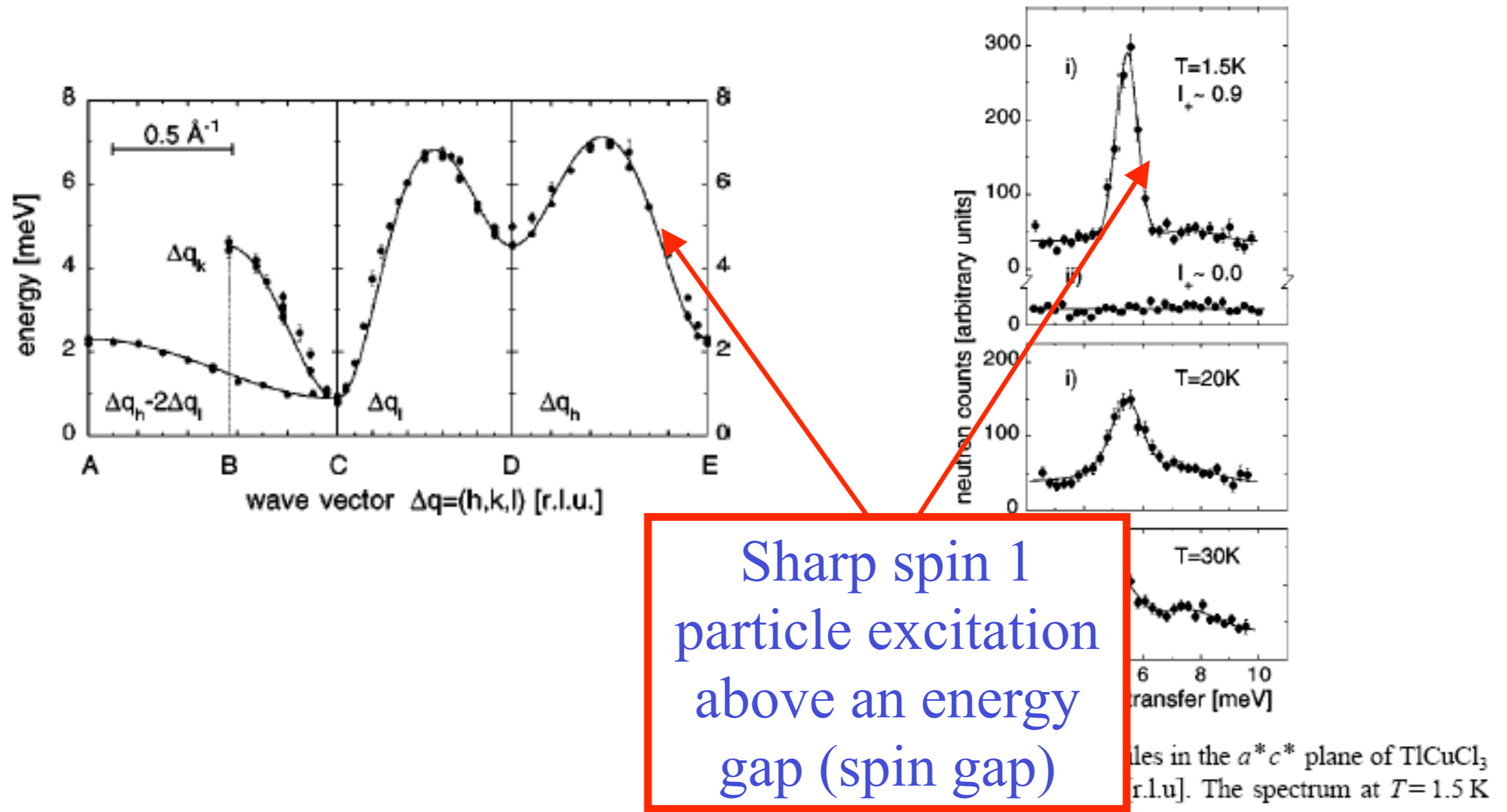


Excitation spectrum in the paramagnetic phase



Sharp spin 1
particle excitation
above an energy
gap (spin gap)

TlCuCl₃ at ambient pressure

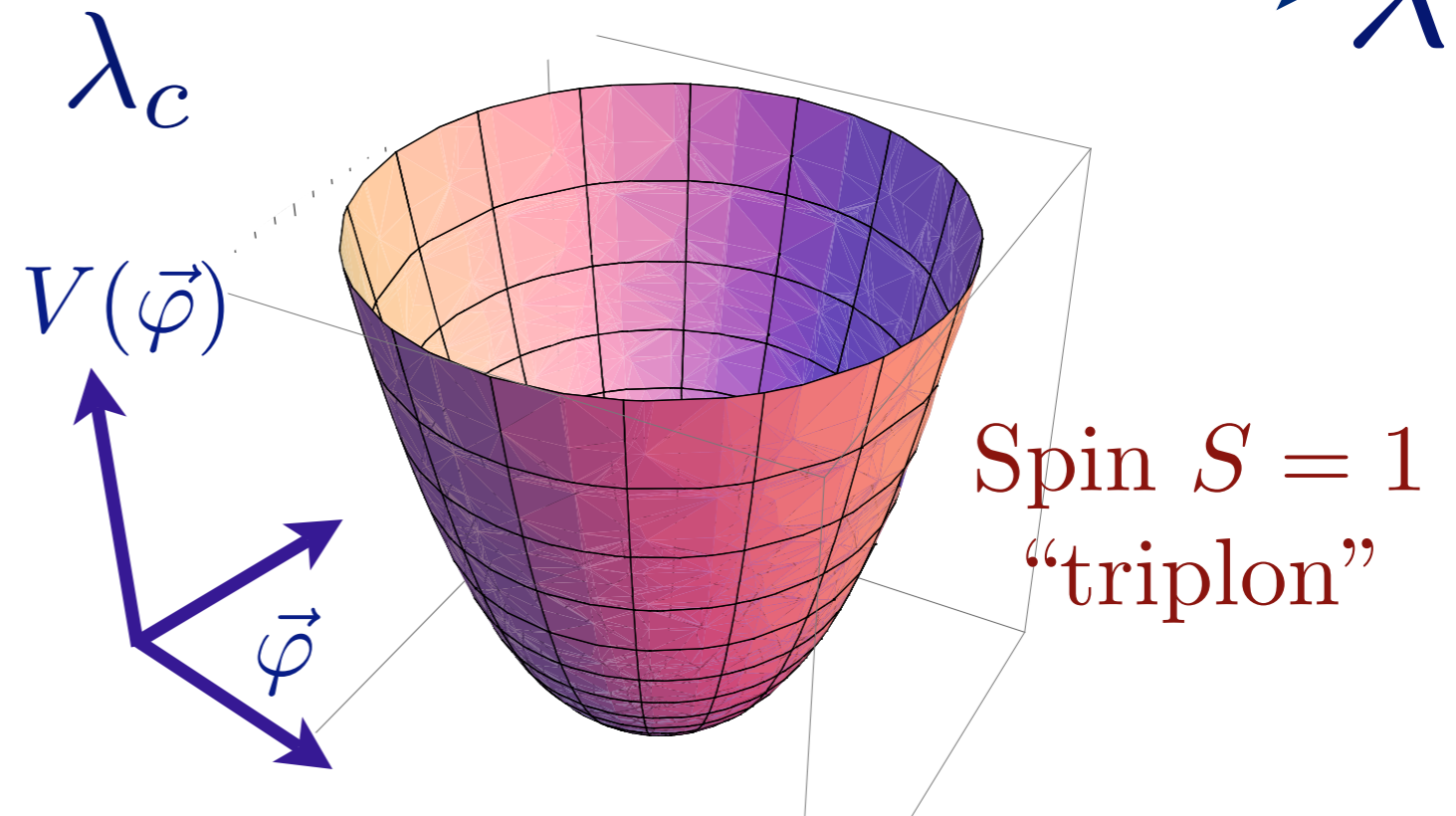
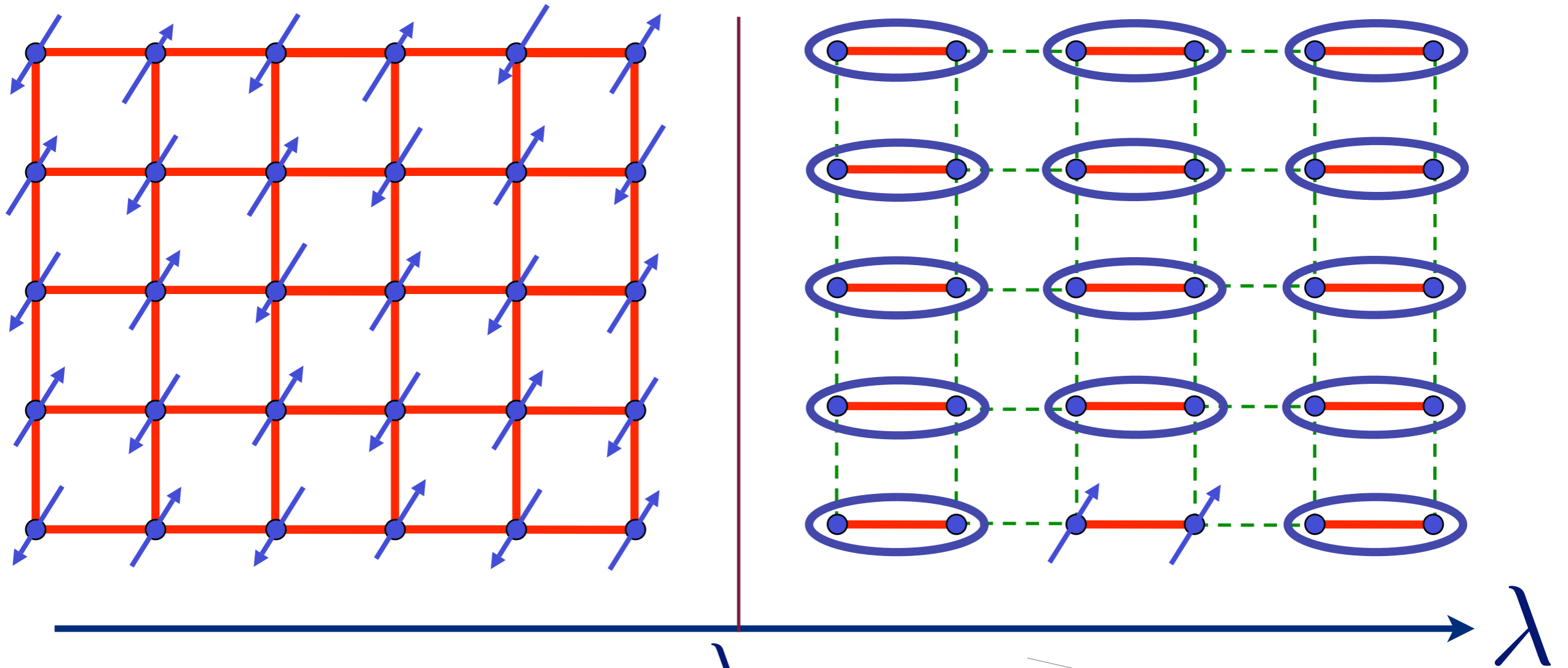


N. Cavadini, G. Heigold, W. Henggeler, A. Furrer, H.-U. Güdel, K. Krämer
and H. Mutka, *Phys. Rev. B* 63 172414 (2001).

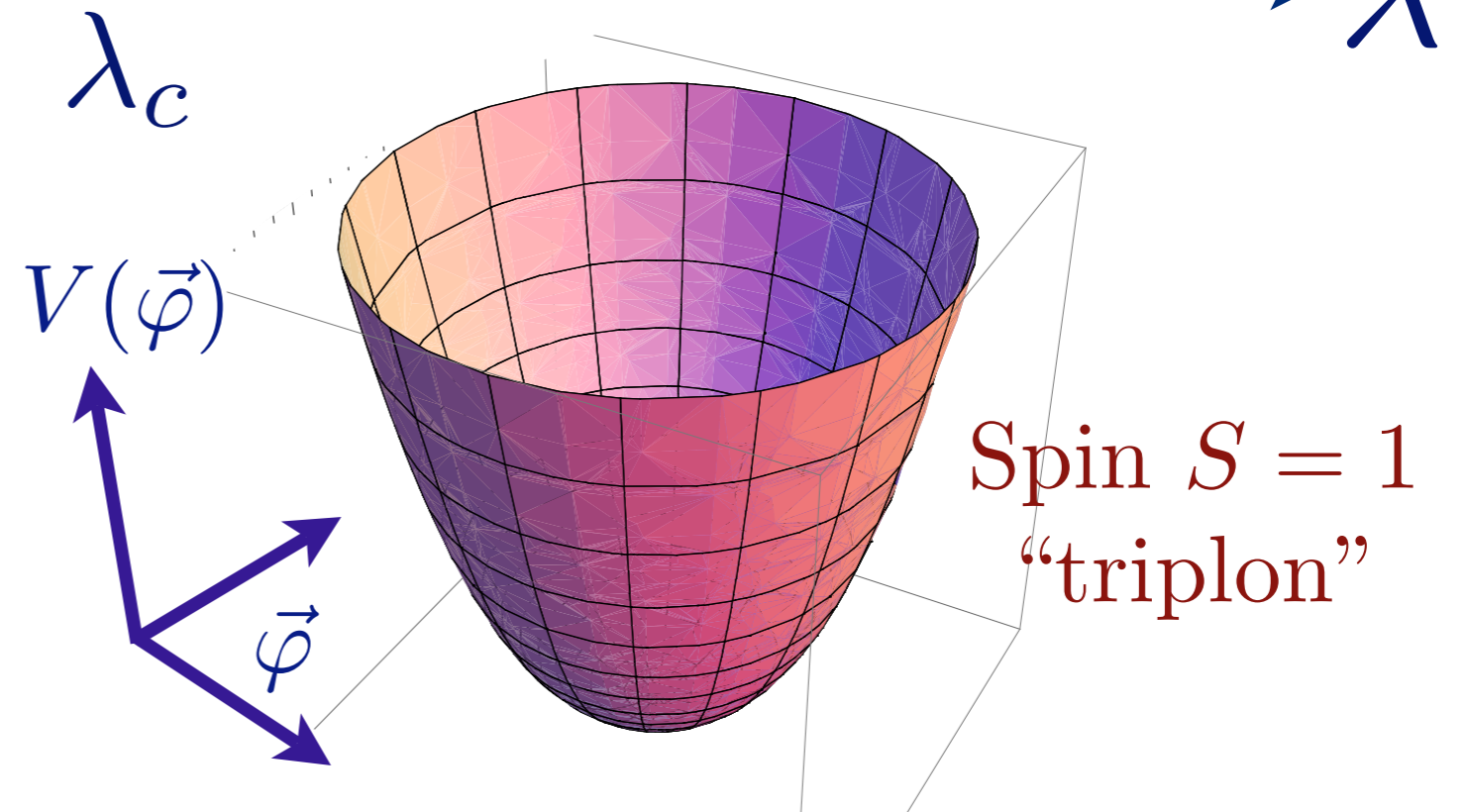
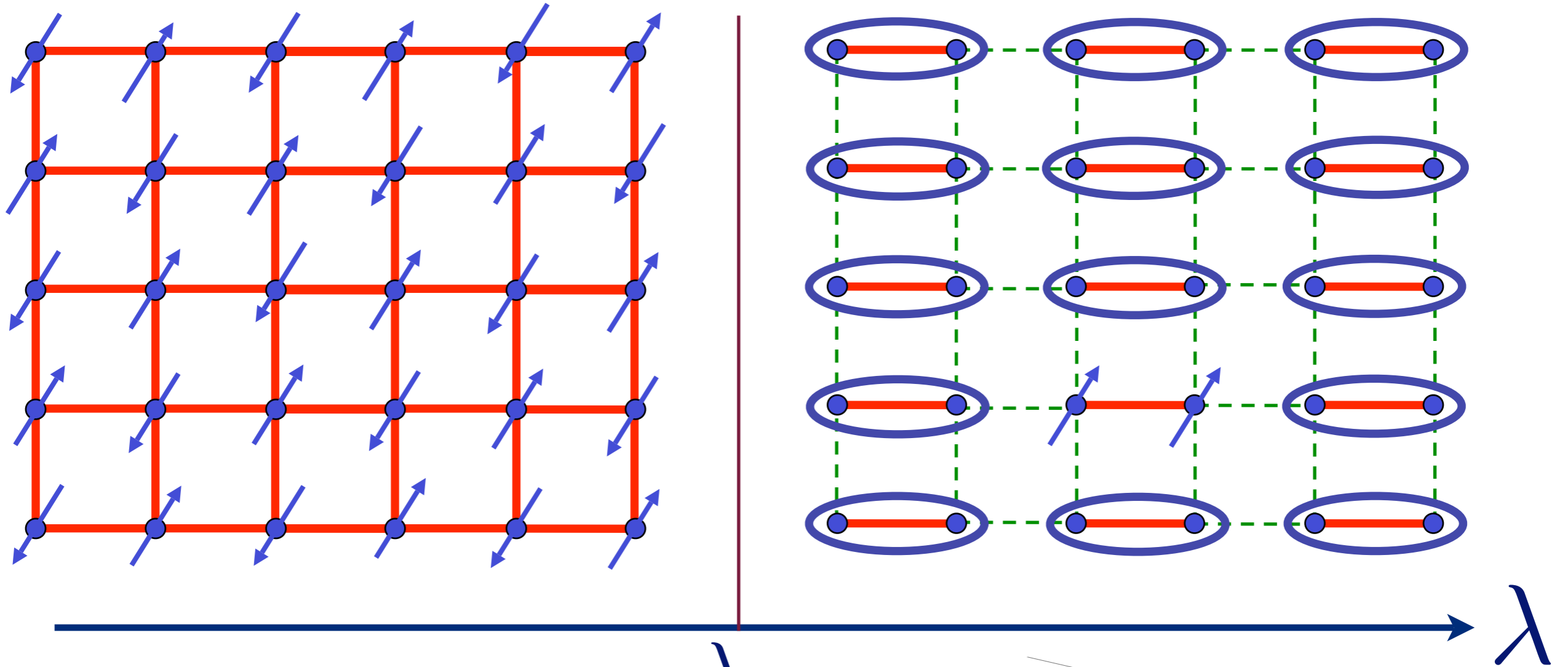
Discussion of bond operator method

<http://qpt.physics.harvard.edu/leshouches/bondoperators.pdf>

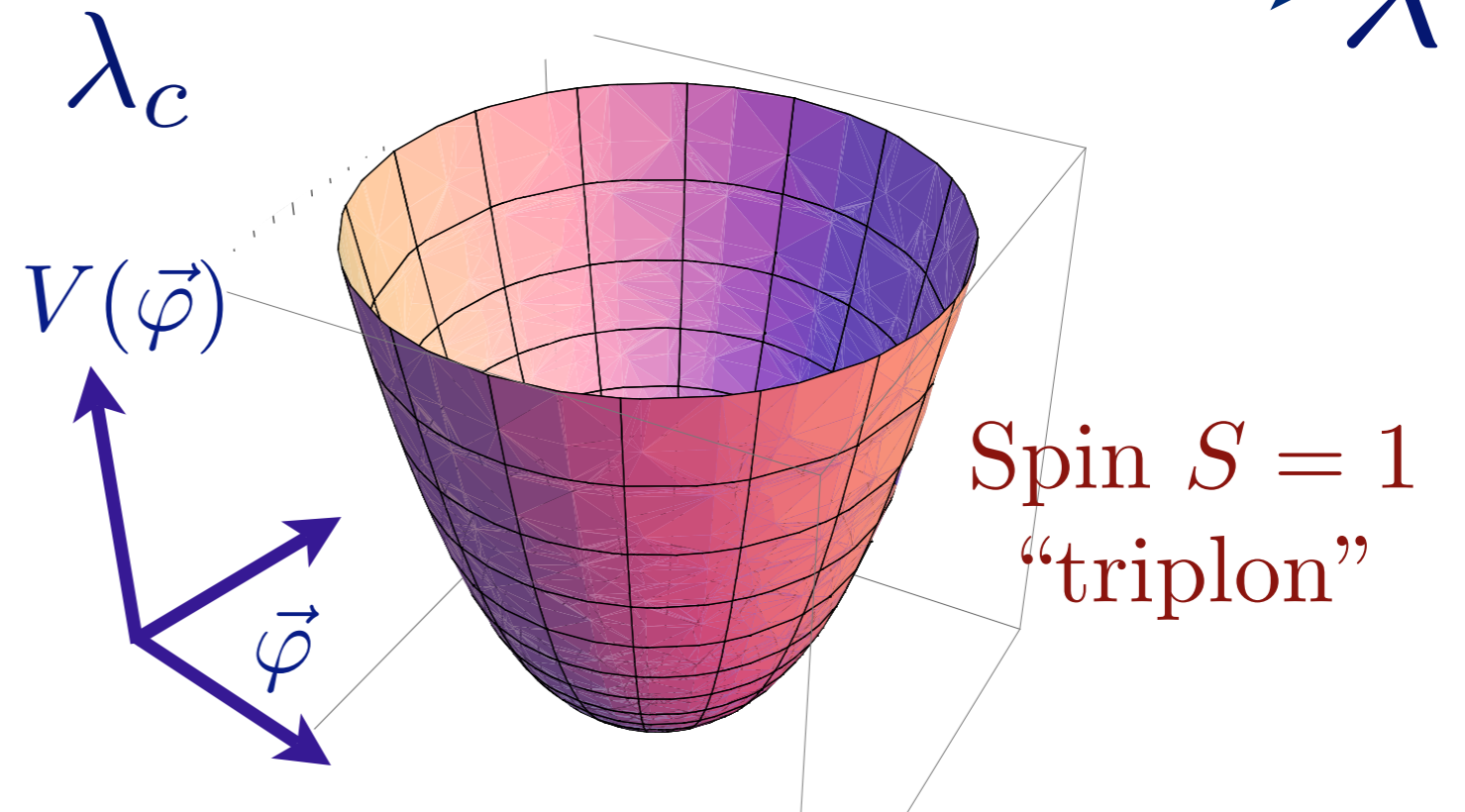
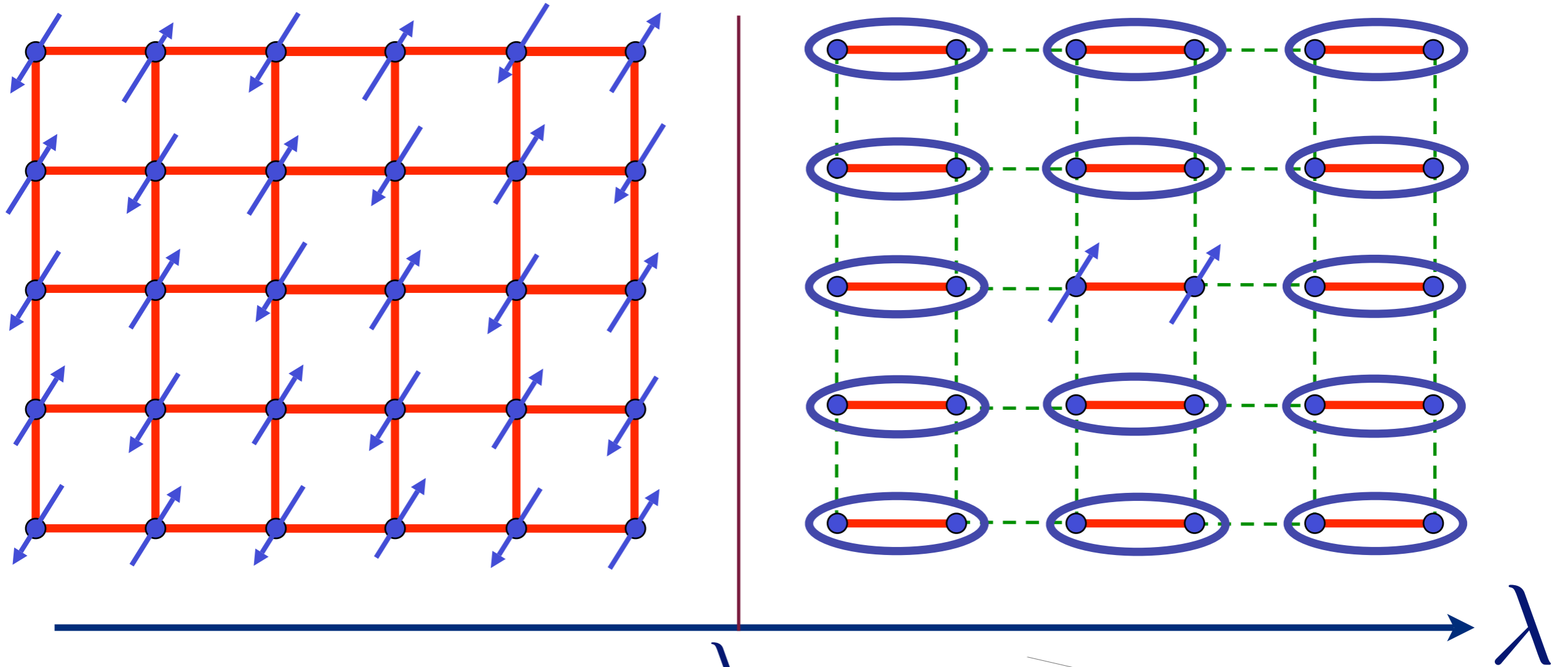
Excitation spectrum in the paramagnetic phase



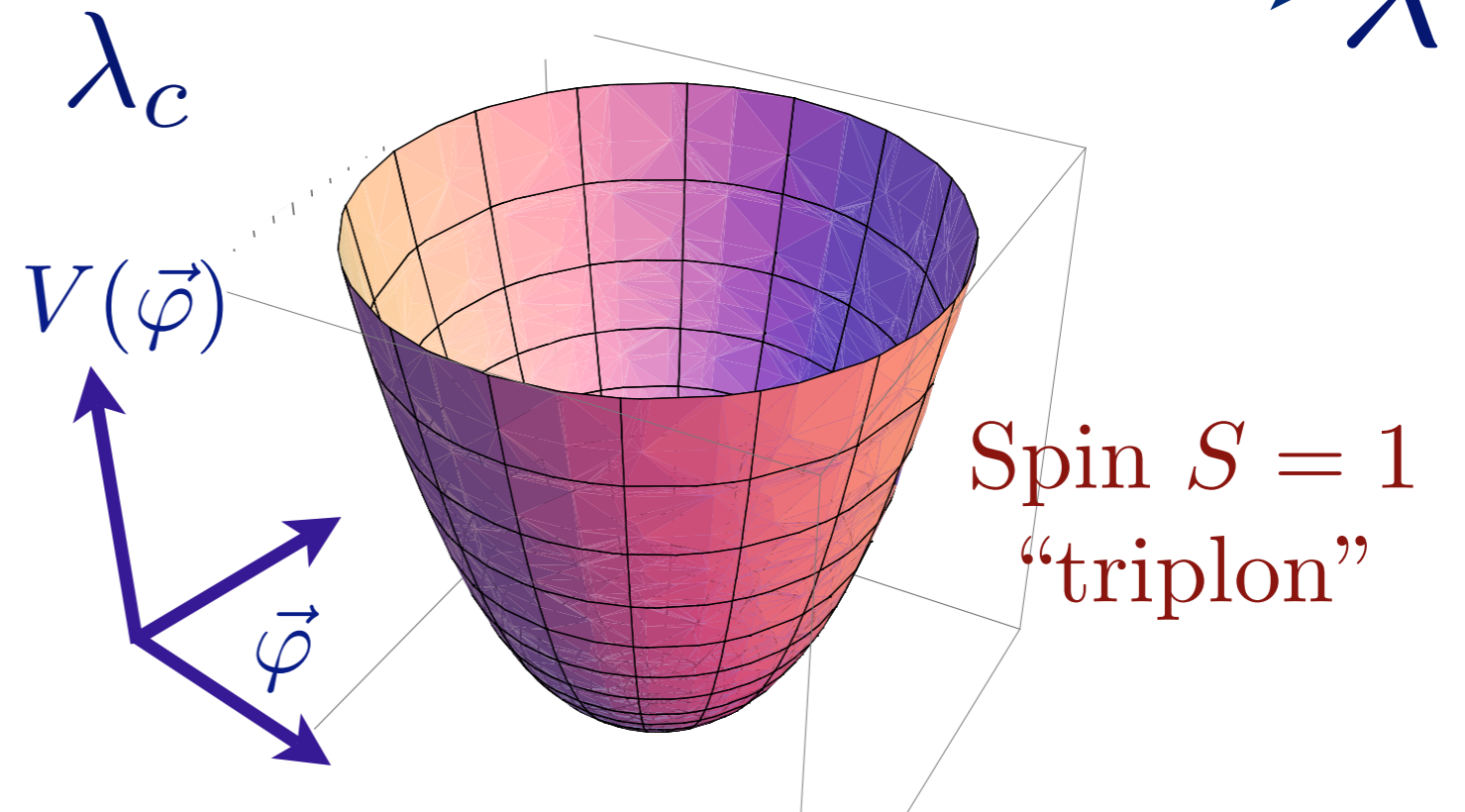
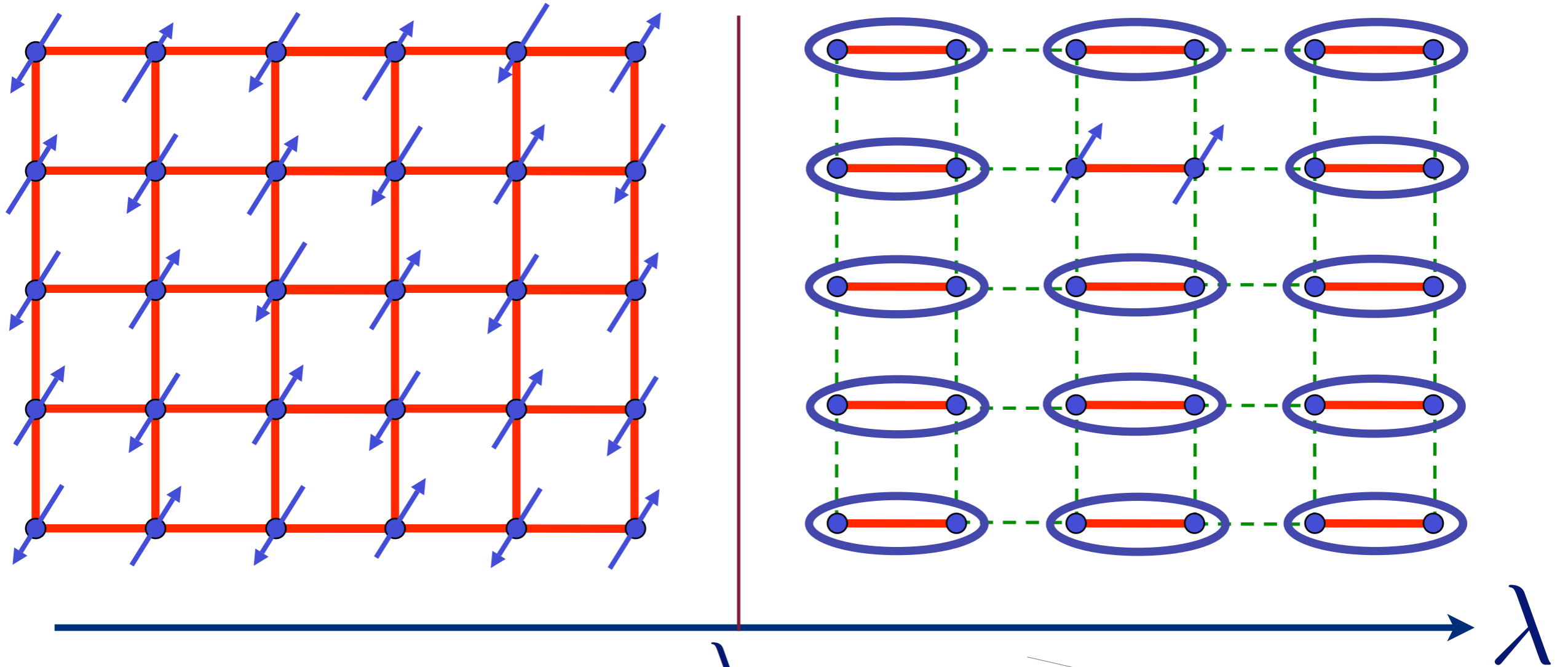
Excitation spectrum in the paramagnetic phase



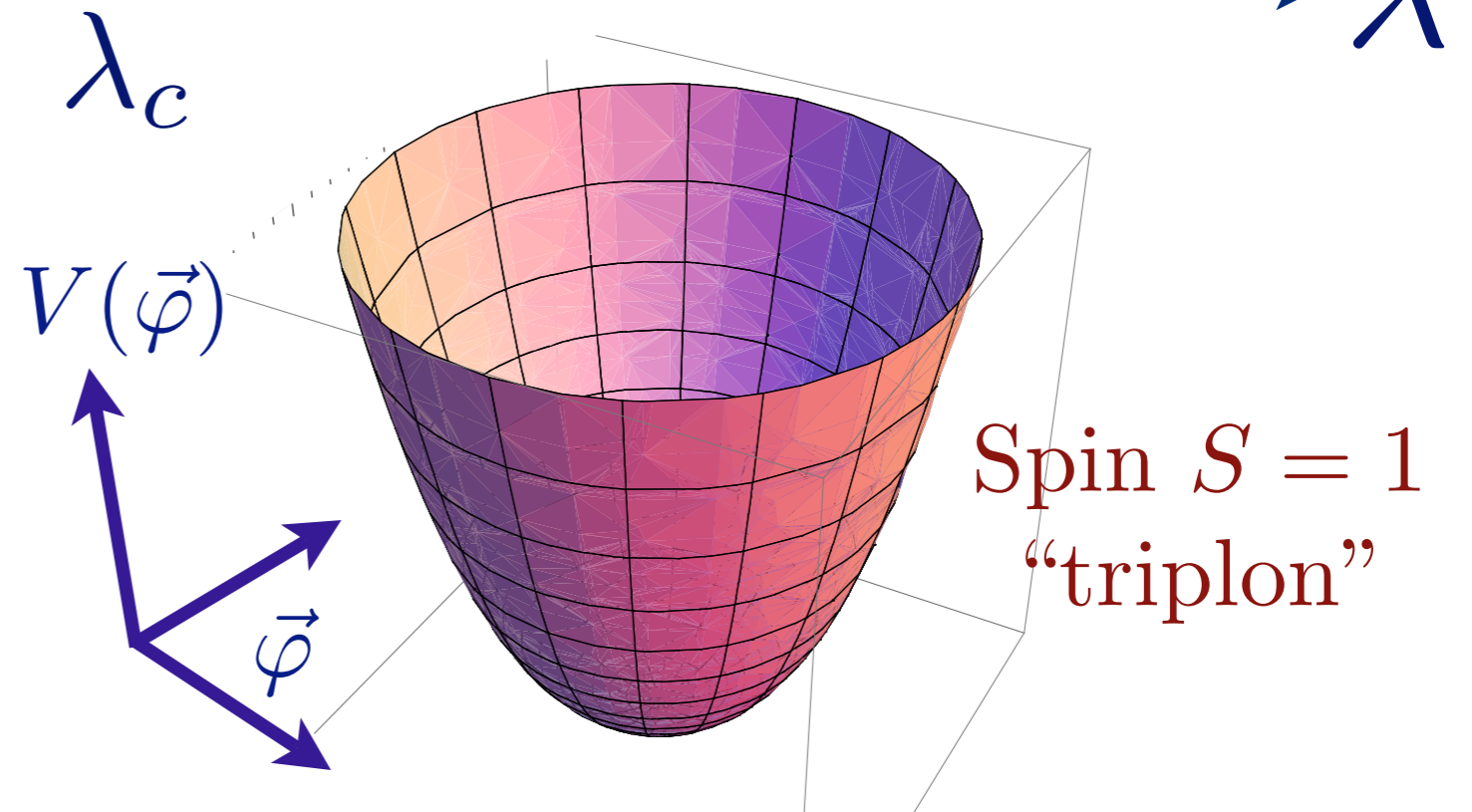
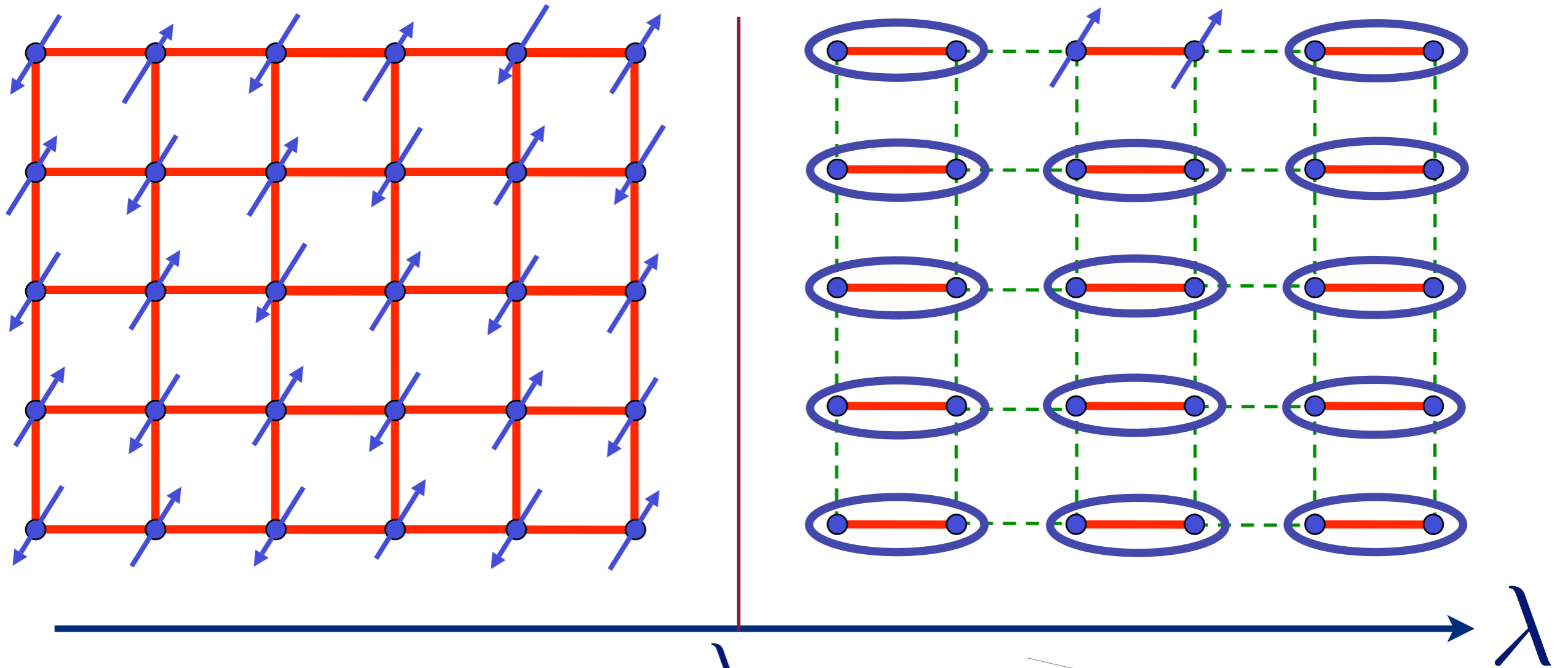
Excitation spectrum in the paramagnetic phase



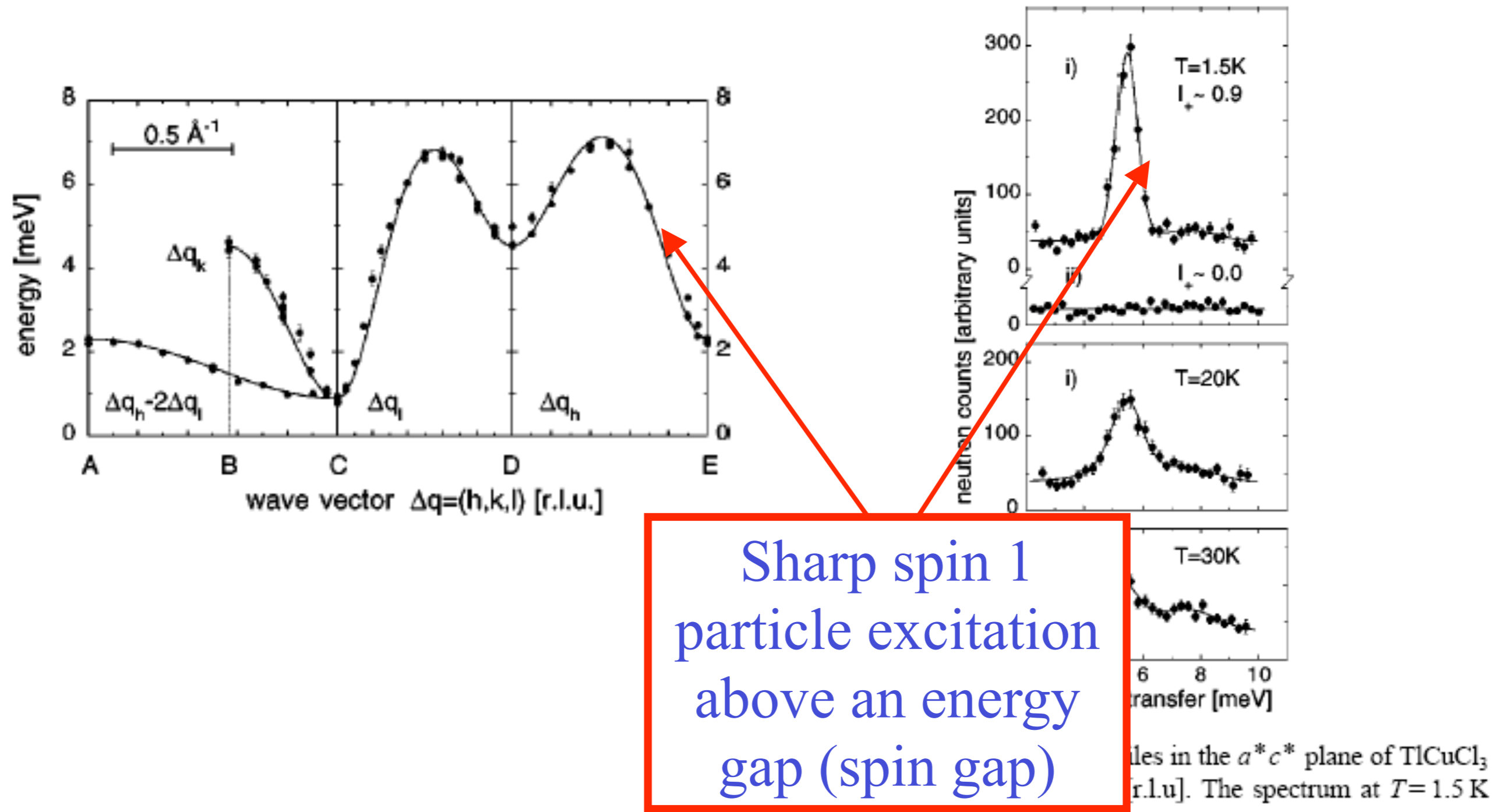
Excitation spectrum in the paramagnetic phase



Excitation spectrum in the paramagnetic phase

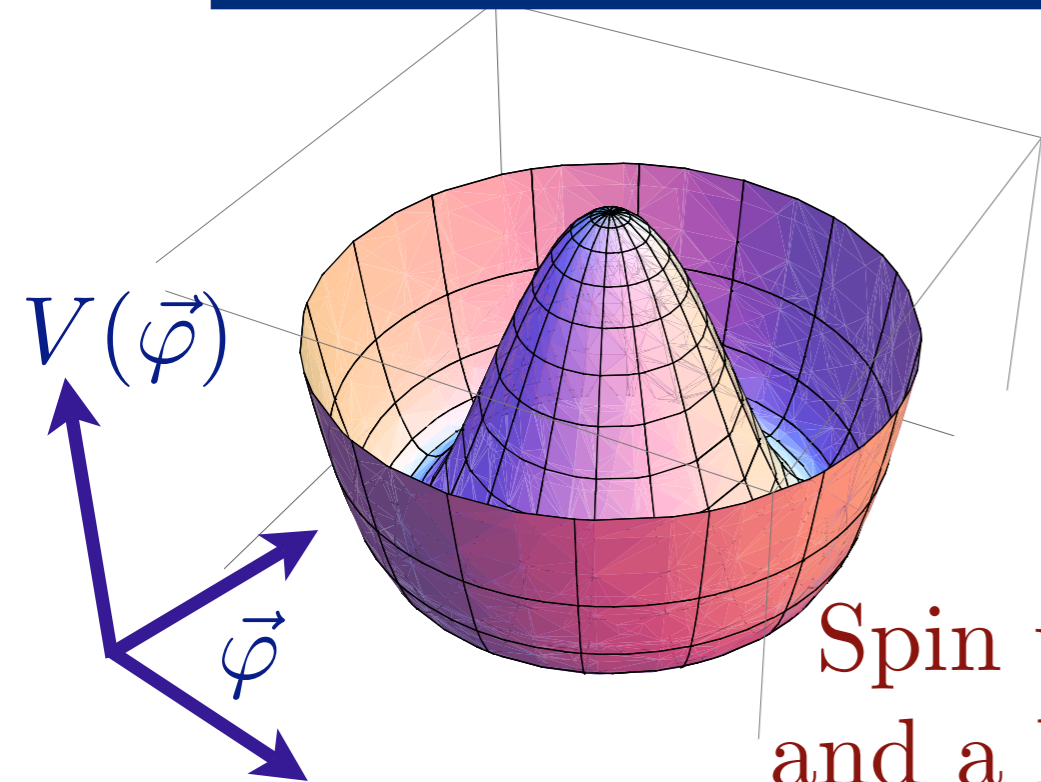
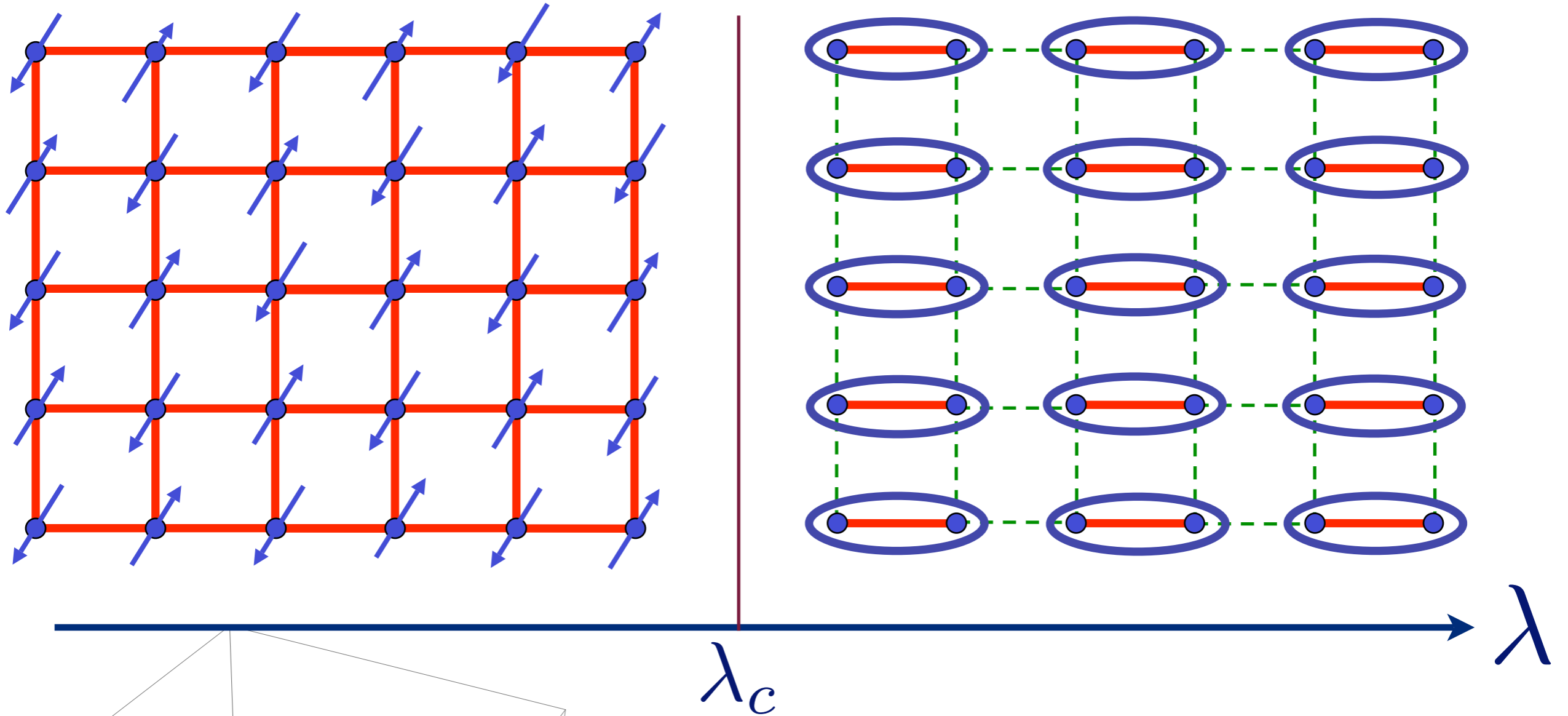


TlCuCl₃ at ambient pressure



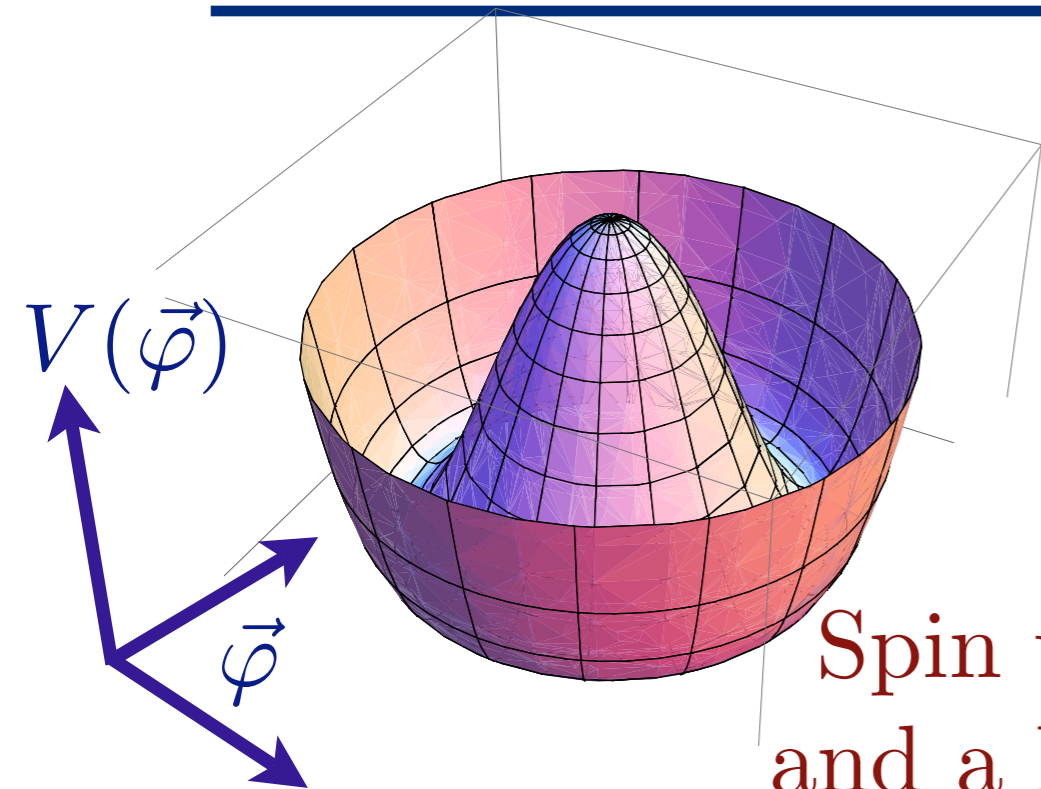
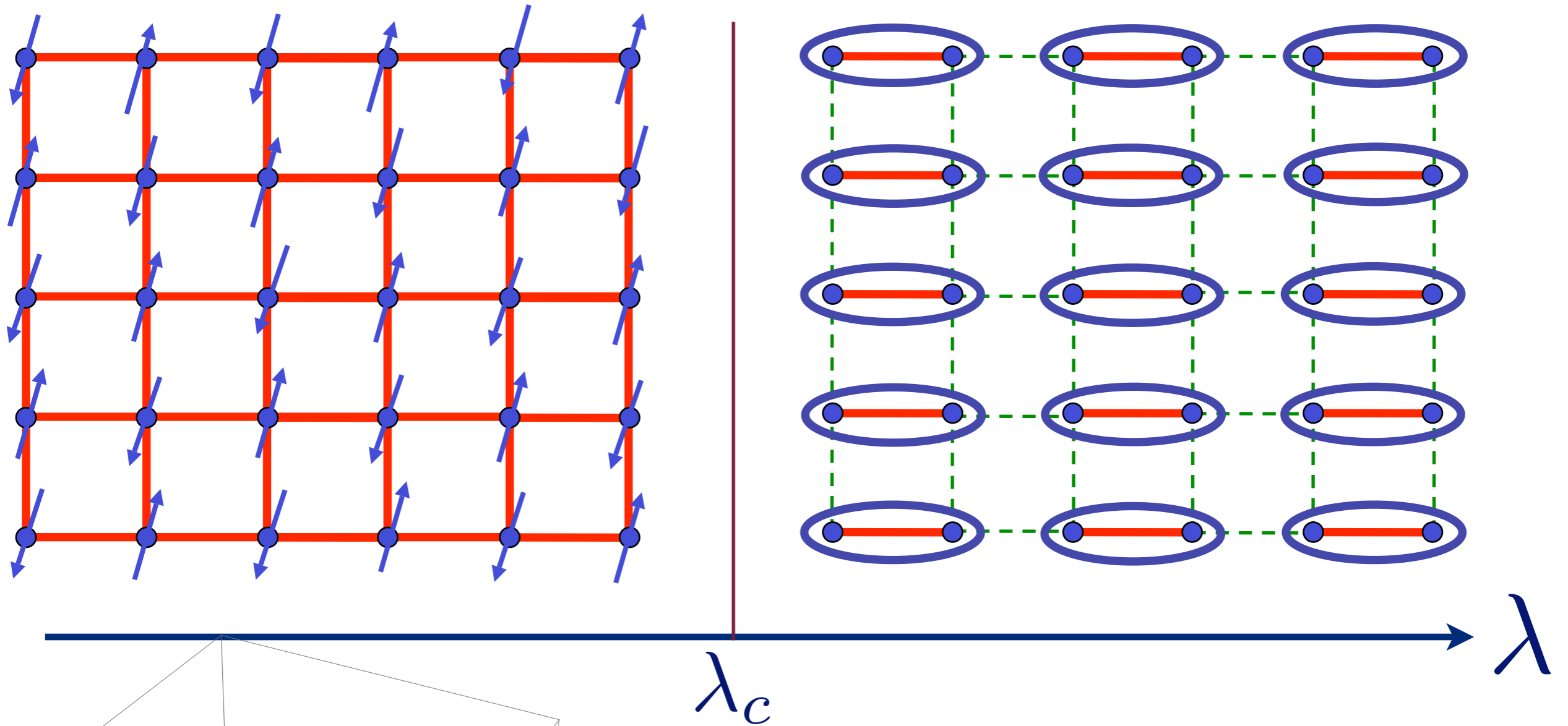
N. Cavadini, G. Heigold, W. Henggeler, A. Furrer, H.-U. Güdel, K. Krämer
and H. Mutka, *Phys. Rev. B* 63 172414 (2001).

Excitation spectrum in the Néel phase



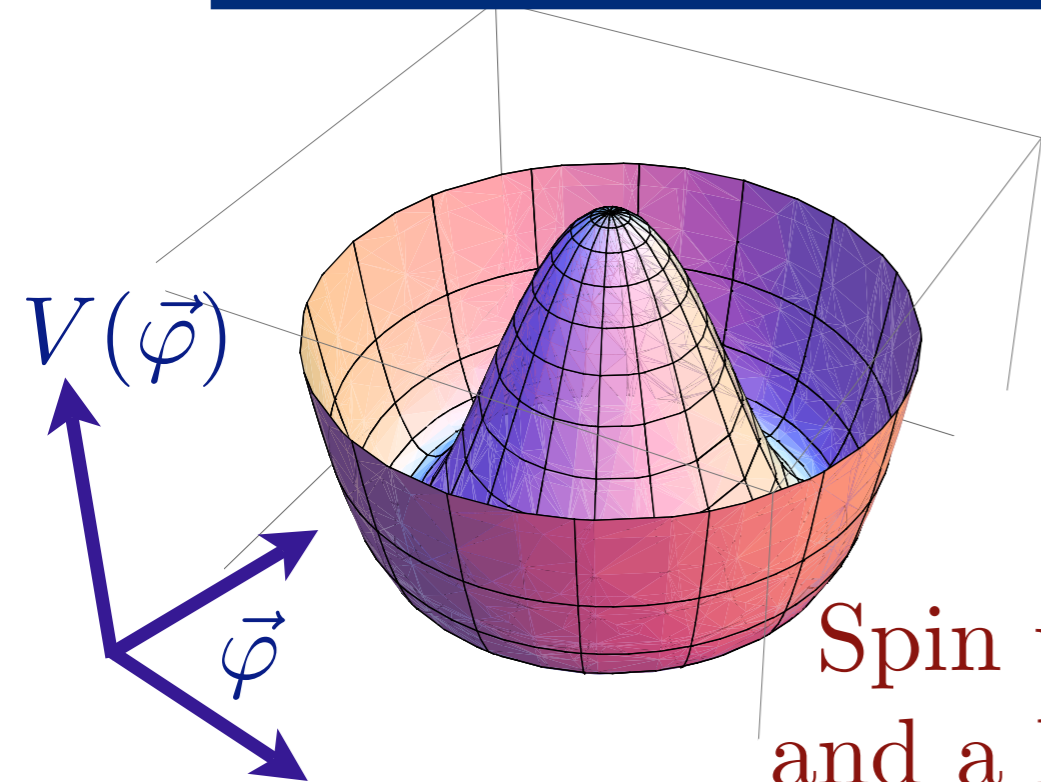
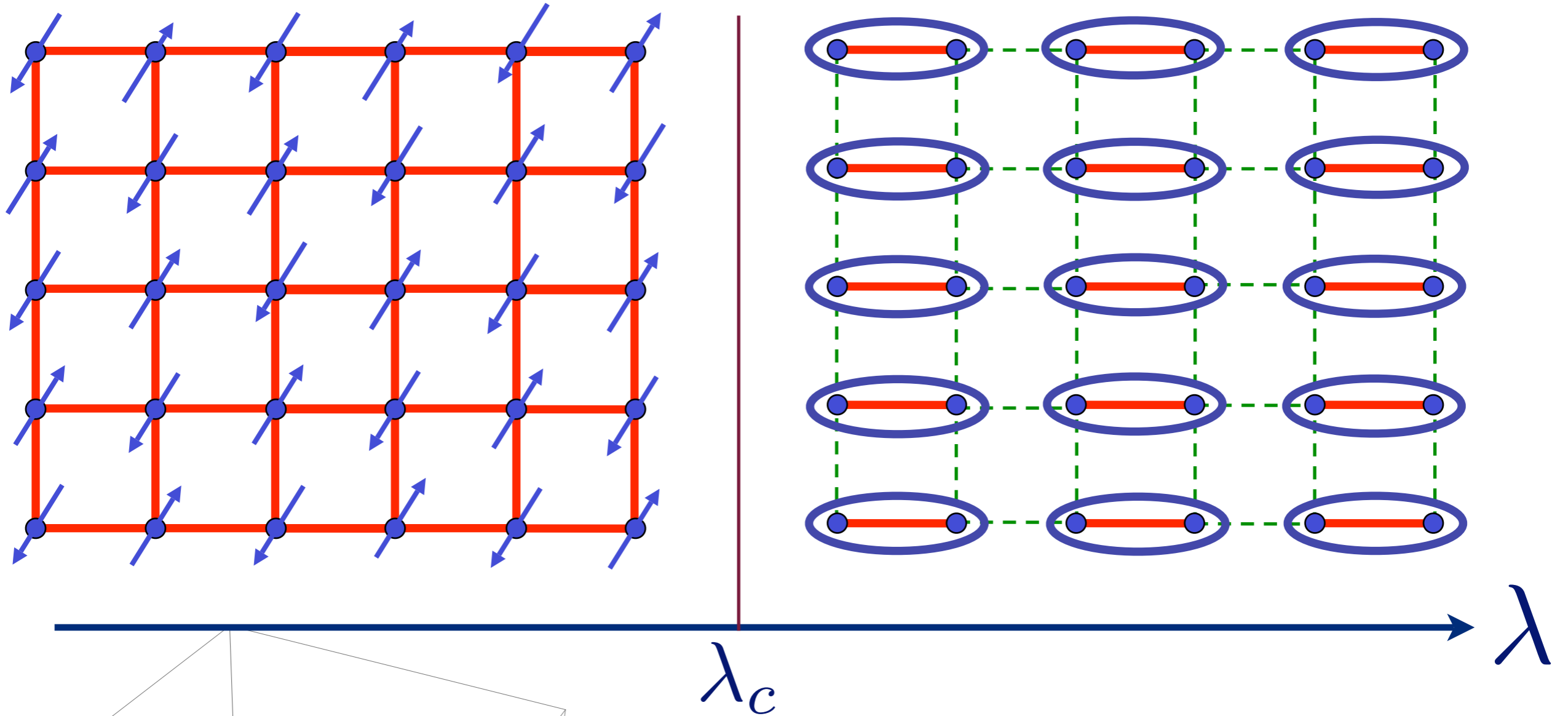
Spin waves (“Goldstone” modes)
and a longitudinal “Higgs” particle

Excitation spectrum in the Néel phase



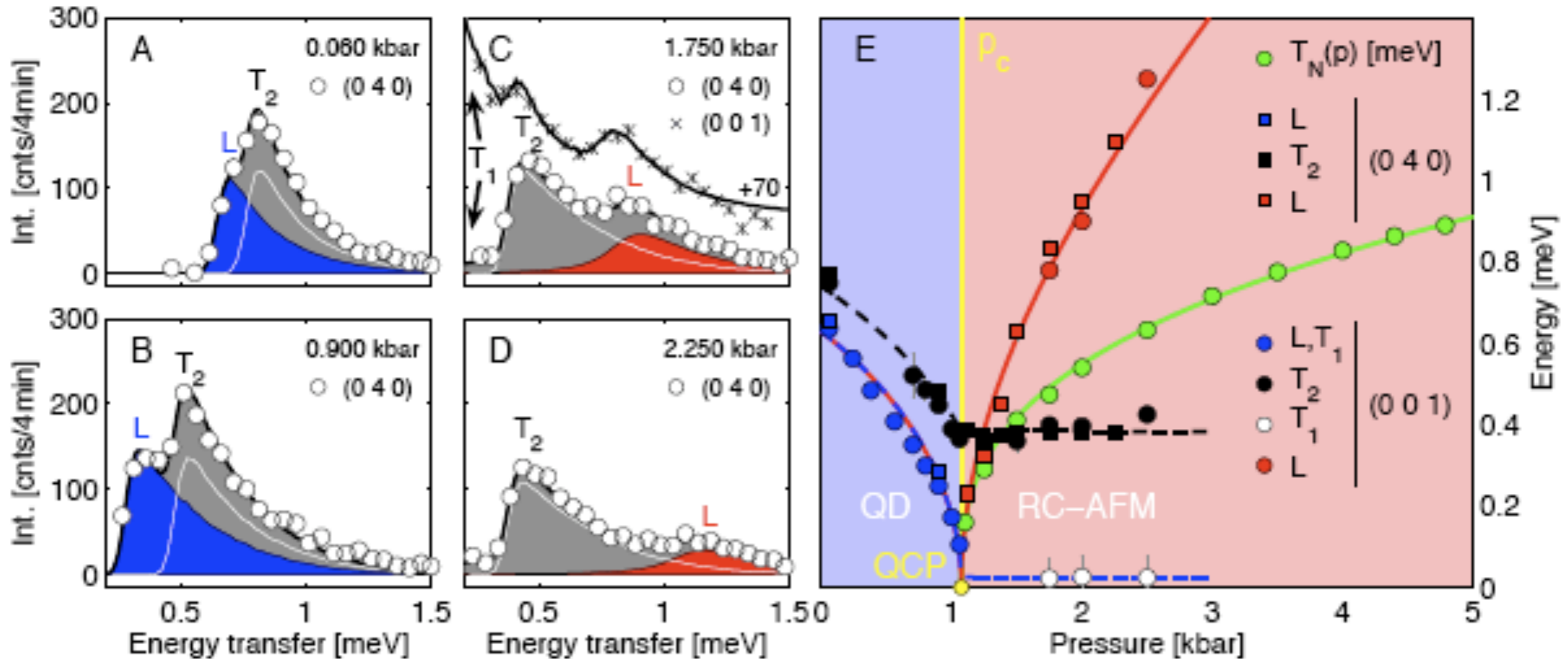
Spin waves (“Goldstone” modes)
and a longitudinal “Higgs” particle

Excitation spectrum in the Néel phase



Spin waves (“Goldstone” modes)
and a longitudinal “Higgs” particle

TiCuCl₃ with varying pressure

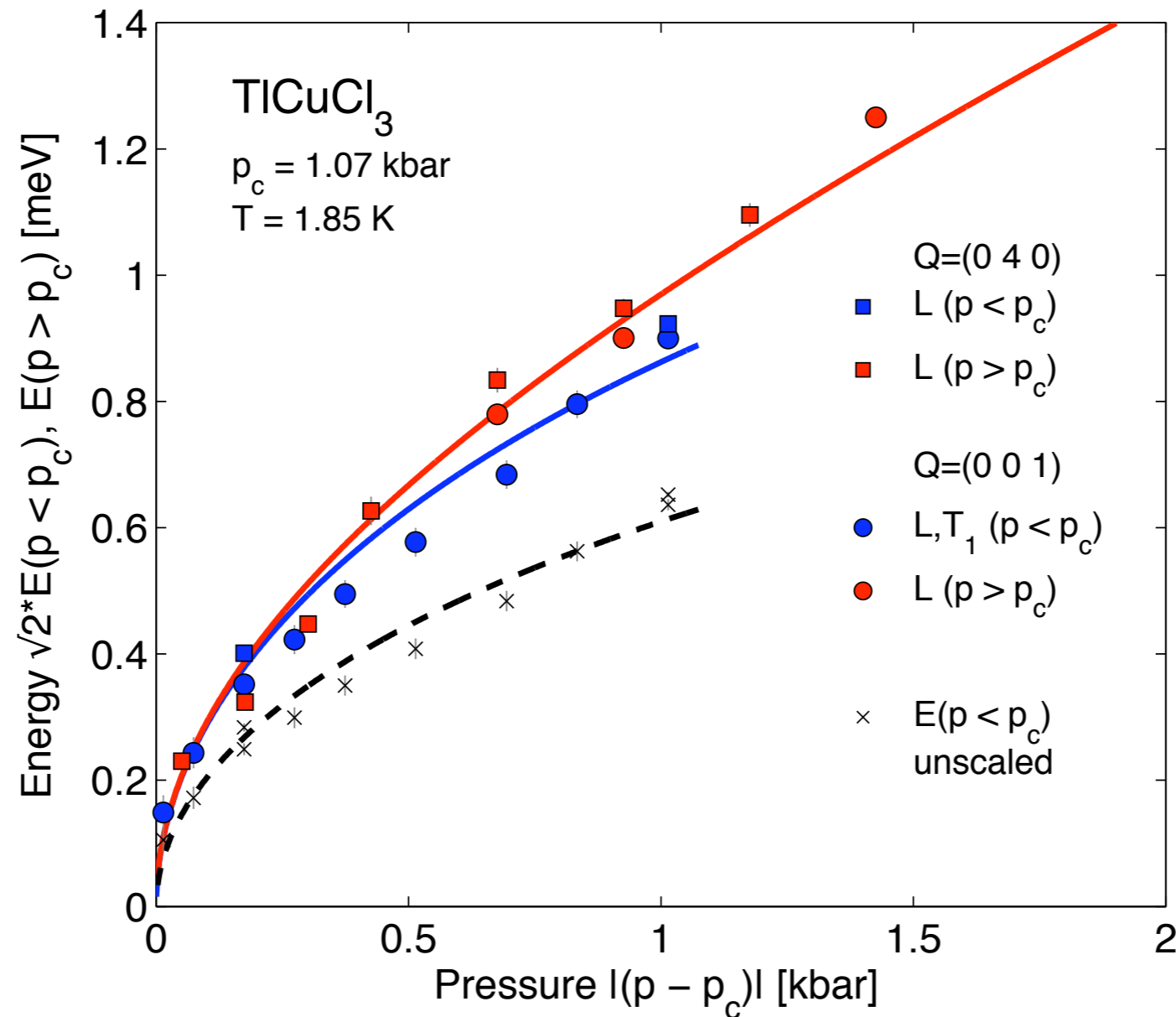


Observation of 3 → 2 low energy modes, emergence of new longitudinal mode (the “Higgs boson”) in Néel phase, and vanishing of Néel temperature at quantum critical point

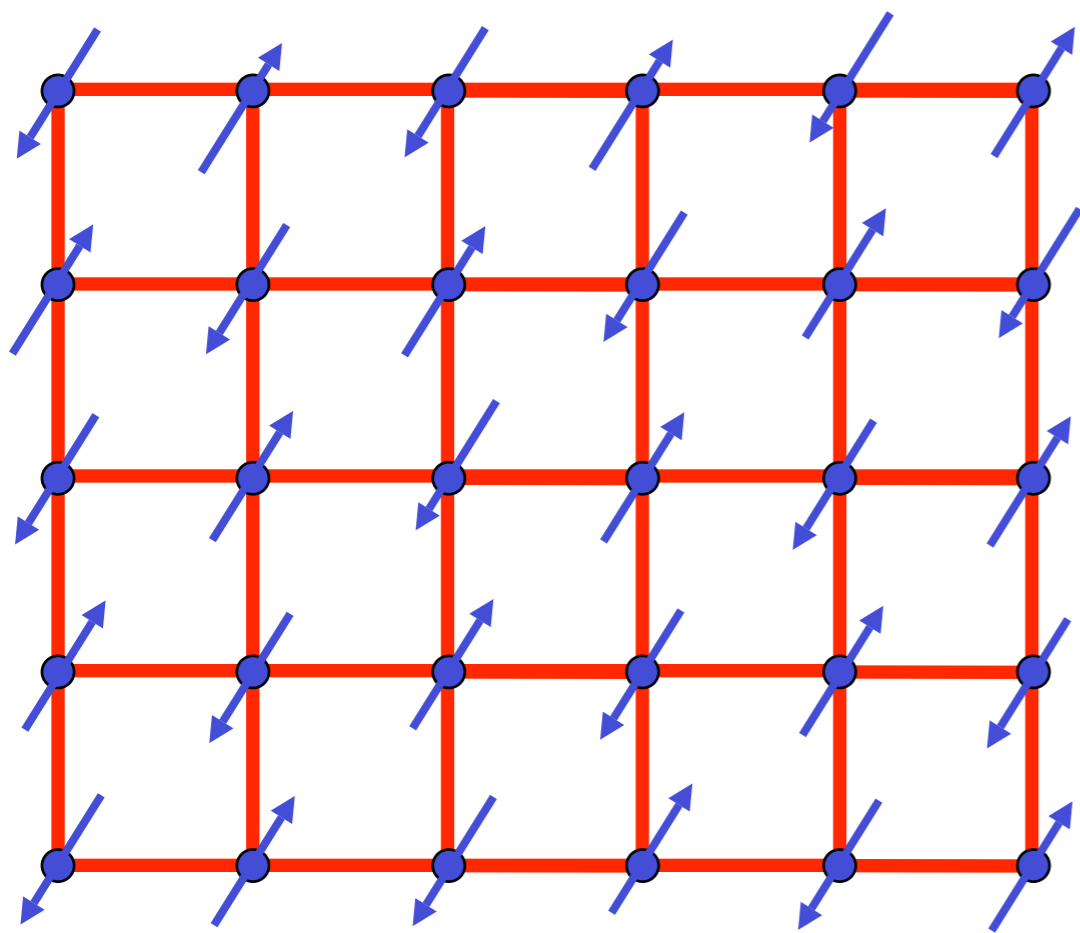
Christian Ruedg, Bruce Normand, Masashige Matsumoto, Albert Furrer, Desmond McMorro, Karl Kramer, Hans-Ulrich Gudel, Severian Gvasaliya, Hannu Mutka, and Martin Boehm, *Phys. Rev. Lett.* **100**, 205701 (2008)

Prediction of quantum field theory

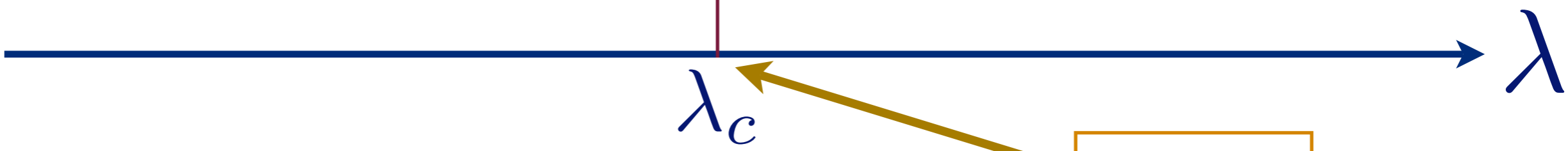
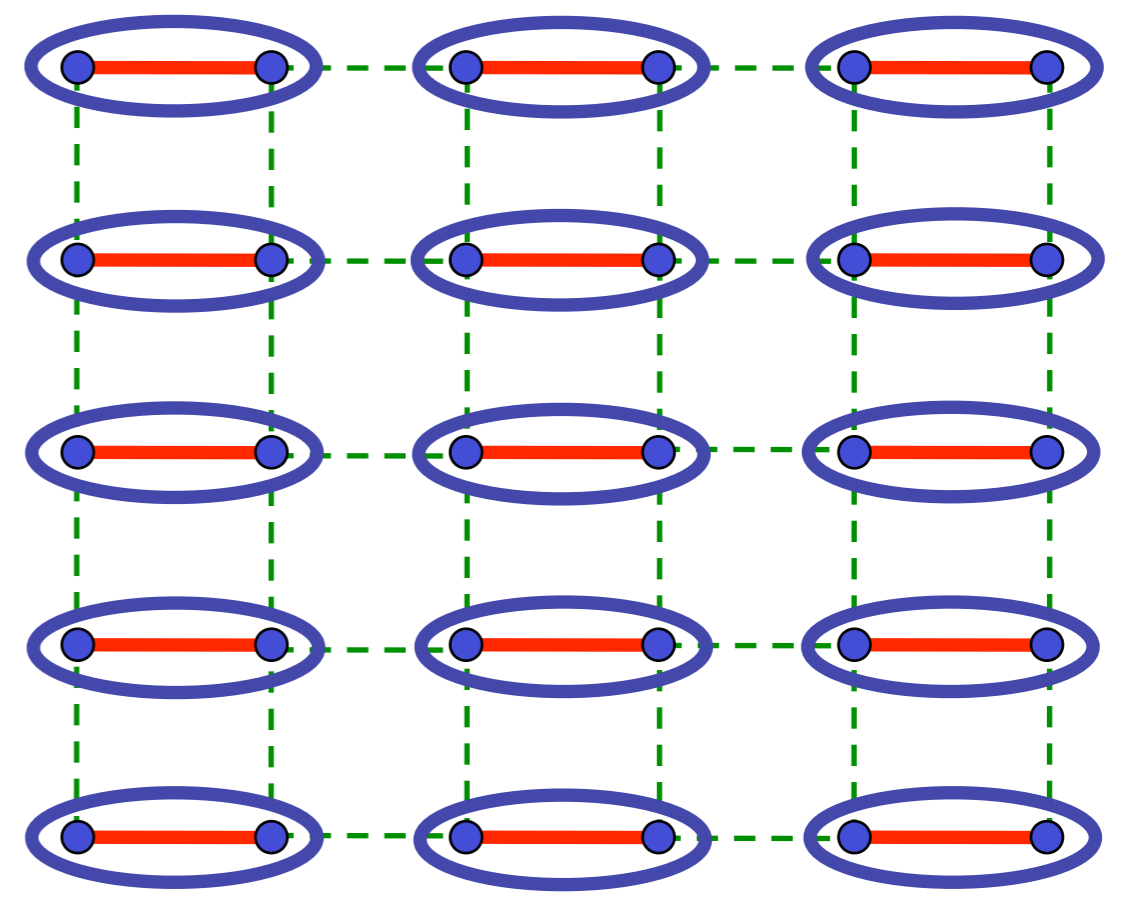
$$\frac{\text{Energy of "Higgs" particle}}{\text{Energy of triplon}} = \sqrt{2}$$



Christian Ruegg, Bruce Normand, Masashige Matsumoto, Albert Furrer, Desmond McMorrow, Karl Kramer, Hans-Ulrich Gudel, Severian Gvasaliya, Hannu Mutka, and Martin Boehm, *Phys. Rev. Lett.* **100**, 205701 (2008)



$$\begin{aligned}
 & \text{Diagram of two blue dots in a blue oval} \\
 & = \frac{1}{\sqrt{2}} (|\uparrow\downarrow\rangle - |\downarrow\uparrow\rangle)
 \end{aligned}$$



$O(3)$ order parameter $\vec{\varphi}$

CFT3

$$\mathcal{S} = \int d^2r d\tau \left[(\partial_\tau \varphi)^2 + c^2 (\nabla_r \vec{\varphi})^2 + s \vec{\varphi}^2 + u (\vec{\varphi}^2)^2 \right]$$

Quantum Monte Carlo - critical exponents

Table IV: Fit results for the critical exponents ν , β/ν , and η . We summarize results including a variation of the critical point within its error bar. For the ladder model (top group of values) fit results and quality of fits are also given at the previous best estimate of α_c . The bottom group are results for the plaquette model. Numbers in [...] brackets denote the $\chi^2/\text{d.o.f.}$ For comparison relevant reference values for the 3D $O(3)$ universality class are given in the last line.

α_c	ν^a	β/ν^b	η^c
1.9096 $-\sigma$	0.712(4) [1.8]	0.516(2) [0.5]	0.026(2) [0.2]
1.9096	0.711(4) [1.8]	0.518(2) [1.1]	0.029(5) [0.8]
1.9096 $+\sigma$	0.710(4) [1.8]	0.519(3) [2.5]	0.032(7) [1.4]
1.9107 ^d	0.709(3) [1.7]	0.525(8) [15.3]	0.051(10) [12]
1.8230 $-\sigma$	0.708(4) [0.99]	0.515(2) [0.84]	0.025(4) [0.15]
1.8230	0.706(4) [1.04]	0.516(2) [0.40]	0.028(3) [0.31]
1.8230 $+\sigma$	0.706(4) [1.10]	0.517(2) [1.6]	0.031(5) [0.80]
Ref. 49	0.7112(5)	0.518(1)	0.0375(5)

^a $L > 12$.

^b $L > 16$.

^c $L > 20$.

^dPrevious best estimate of Ref. 19.

S. Wenzel and W. Janke, arXiv:0808.1418

M. Troyer, M. Imada, and K. Ueda, *J. Phys. Soc. Japan* (1997)

Quantum Monte Carlo - critical exponents

Table IV: Fit results for the critical exponents ν , β/ν , and η . We summarize results including a variation of the critical point within its error bar. For the ladder model (top group of values) fit results and quality of fits are also given at the previous best estimate of α_c . The bottom group are results for the plaquette model. Numbers in [...] brackets denote the $\chi^2/\text{d.o.f.}$ For comparison relevant reference values for the 3D $O(3)$ universality class are given in the last line.

α_c	ν^a	β/ν^b	η^c
1.9096 $-\sigma$	0.712(4) [1.8]	0.516(2) [0.5]	0.026(2) [0.2]
1.9096	0.711(4) [1.8]	0.518(2) [1.1]	0.029(5) [0.8]
1.9096 $+\sigma$	0.710(4) [1.8]	0.519(3) [2.5]	0.032(7) [1.4]
1.9107 ^d	0.709(3) [1.7]	0.525(8) [15.3]	0.051(10) [12]
1.8230 $-\sigma$	0.708(4) [0.99]	0.515(2) [0.84]	0.025(4) [0.15]
1.8230	0.706(4) [1.04]	0.516(2) [0.40]	0.028(3) [0.31]
1.8230 $+\sigma$	0.706(4) [1.10]	0.517(2) [1.6]	0.031(5) [0.80]
Ref. 49	0.7112(5)	0.518(1)	0.0375(5)

Field-theoretic
RG of CFT3
E.Vicari *et al.*

^a $L > 12$.

^b $L > 16$.

^c $L > 20$.

^dPrevious best estimate of Ref. 19.

S. Wenzel and W. Janke, arXiv:0808.1418

M. Troyer, M. Imada, and K. Ueda, *J. Phys. Soc. Japan* (1997)